M.Tech (Power Electronics and Systems)

Anurag Singh

2024

Performance Analysis of Single Phase and Three Phase Inductive Power Transfer based Wireless Charging

A DISSERTATION

SUBMITTED IN PARTIAL FULFILLMENT OF THE REQUIREMENTS

FOR THE AWARD OF THE DEGREE

OF

MASTER OF TECHNOLOGY

IN

POWER ELECTRONICS AND SYSTEMS

Submitted by:

ANURAG SINGH

2K22/PES/04

Under the supervision of

PROF. MUKHTIAR SINGH

(Professor, EED, DTU)

DEPARTMENT OF ELECTRICAL ENGINEERING

DELHI TECHNOLOGICAL UNIVERSITY

(Formerly Delhi College of Engineering)

Bawana Road, Delhi-110042

MAY, 2024

DEPARTMENT OF ELECTRICAL ENGINEERING

DELHI TECHNOLOGICAL UNIVERSITY

(Formerly Delhi College of Engineering)

Bawana Road, Delhi-110042

CANDIDATE'S DECLARATION

I, Anurag Singh, Roll No. 2K22/PES/04 student of MTech (Power Electronics & Systems), hereby declare that the project Dissertation titled **"Performance Analysis of Single Phase and Three Phase Inductive Power Transfer based Wireless Charging"** which is submitted by me to the Department of Electrical Engineering, Delhi Technological university, Delhi in partial fulfilment of the requirement for the award of the degree of Master of Technology, is original and not copied from any source without proper citation. This work has not previously formed the basis for the award of any Degree, Diploma Associateship, Fellowship, or other similar title or recognition.

Place: Delhi **(Anurag Singh)**

Date: 7th June 2024

DEPARTMENT OF ELECTRICAL ENGINEERING

DELHI TECHNOLOGICAL UNIVERSITY

(Formerly Delhi College of Engineering)

Bawana Road, Delhi-110042

CERTIFICATE

I hereby certify that the project Dissertation titled **"Performance Analysis of Single Phase and Three Phase Inductive Power Transfer based Wireless Charging"** which is Submitted by **Anurag Singh,** Roll No. **2K22/PES/04**, Department of Electrical Engineering, Delhi Technological University, Delhi in partial fulfilment of the requirement for the award of the degree of Master of Technology, is a record of the project work carried out by the student under my supervision. To the best of my knowledge, this work has not been submitted in part or full for any Degree or Diploma to this University or elsewhere.

Place: Delhi

Date: 7th June 2024

PROF. MUKHTIAR SINGH

(SUPERVISOR)

DEPARTMENT OF ELECTRICAL ENGINEERING

DELHI TECHNOLOGICAL UNIVERSITY

(Formerly Delhi College of Engineering)

Bawana Road, Delhi-110042

ACKNOWLEDGEMENT

I would like to express my gratitude towards all the people who have contributed their precious time and effort to help me without whom it would not have been possible for me to understand and complete the project. I would like to thank **Prof. Mukhtiar Singh, DTU Delhi, Department of Electrical Engineering**, my Project Supervisor, for supporting, motivating, and encouraging me throughout this work was carried out. His readiness for consultation at all times, his educative comments, and his concern and assistance even with practical things have been invaluable.

Besides my supervisor, I would like to thank **Mr. Gaurav Yadav** (Ph.D. scholar) and all the Ph.D. scholars of PE LAB for helping me wherever required and providing me with continuous motivation during my research.

Finally, I must express my very profound gratitude to my parents, seniors, and my friends for providing me with unfailing support and continuous encouragement throughout the research work.

Date: 7th June 2024

Anurag Singh

M.tech (Power Electronics & Systems)

Roll No. 2K22/PES/04

ABSTRACT

Wireless battery charging technology has the potential to enhance the ease and sustainability of electric vehicles (EVs) by eliminating the requirement for physical connection to charge. This study presents a new wireless battery charger specifically built for electric vehicle (EV) applications. The charger obtains electricity from the AC grid to perform power factor correction and enable wireless charging. The charger utilizes a complex procedure to convert alternating current (AC) to direct current (DC), then transforms it back to high-frequency AC for wireless power transfer, and lastly rectifies it back to DC. This ensures the charging process is stable and efficient. An Active Front Rectifier is a key component of its operation. It utilizes the three-phase synchronous reference frame theory to effectively maintain voltage stability. This design enables the charger to operate autonomously without a local controller on the vehicle, seamlessly integrating into current infrastructures and improving convenience. The fundamental principle of wireless charging is the utilization of Inductive Power Transfer (IPT) technology, which efficiently transfers power by means of magnetic connection between the charger and the car. Nevertheless, the system's efficiency can be affected by issues such as misalignment of magnetic couplers, which can lead to swings in output power and mutual inductance. In order to tackle these difficulties, scientists have investigated several configurations that have a higher tolerance for misalignment. This has been achieved by making adjustments to the magnetic couplers, compensation networks, and control methods. Each of these alterations has its own benefits, which rely on criteria like as reliability, efficiency, and cost. The research has made major contributions to the area by demonstrating the potential of wireless charging technology to improve the experience of charging electric vehicles. This technology offers increased adaptability, reliability, and efficiency.

TABLE OF CONTENTS

LIST OF FIGURES

LIST OF TABLES

LIST OF ABBREVIATIONS

WPT	Wireless Power Transfer
Rx	Receiver
Tx	Transmitter
M	Mutual inductance
k	Coupling coefficient
EV	Electric vehicle
AV	Autonomous vehicle
RF	Radio frequency
S	Series
P	Parallel
PA	Power Amplifier
SOC	State of charge
VA	Volt-ampere
LCC	Compensation circuit (series inductor, parallel and series capacitors)
LCL	Compensation circuit (series inductor and parallel capacitor)
PTE	Power transfer efficiency
TP	Transferred power
FHA	Fundamental harmonic analysis

Chapter 1

INTRODUCTION

1.1. Background

An outline of WPT systems, their uses, and their accomplishments are presented in this chapter. Additionally, this thesis highlights its objectives, scope, and contributions.

1.1.1. Introduction to Wireless power Transfer

Over a century ago, Nikola Tesla showcased the initial instance of wireless power transmission (WPT) by utilizing electrostatic induction [1]. Progress and developments were limited during that period due to the prevailing technical limits of semiconductor technology. The development of sophisticated semiconductor and winding technology has led to a recent increase in interest in WPT. As shown in Fig. 1.1, a wireless power transfer (WPT) device has two main parts: a transmitting (Tx) unit and a receiving (Rx) unit. The power source for direct current (DC) or alternating current (AC) is connected to the power electronic converter on the sending side. Because of this, the high-frequency AC current is produced. In order to make the Tx coil magnetic, high frequency alternating current is utilized. This ultimately results in the Tx coil being magnetically connected to the Rx coil.

The Tx coil generates a magnetic field that causes voltage to be induced in the Rx coil, allowing electrical energy to be transferred across a predetermined distance through the air. The energy that is delivered wirelessly can be transformed into a form that is appropriate for powering a load. In wireless power transfer (WPT), the conFiguration is akin to that of transformers, In a wireless power transfer (WPT) system, the coils involved have a loose coupling because they are significantly separated. However, a magnetic core is used to enhance the robustness of the coupling between these coils. Due to the low coupling and the inductive nature of the Tx and Rx coils, there is a substantial amount of leakage inductance. Consequently, the total impedance of the system rises. In order to minimize this

impact, It is possible to connect correction circuits to both the sending (Tx) and receiving (Rx) coils. The goal of these circuits is to reduce or get rid of any reactance that isn't needed so that the magnetizing current and magnetic field are as strong as possible.

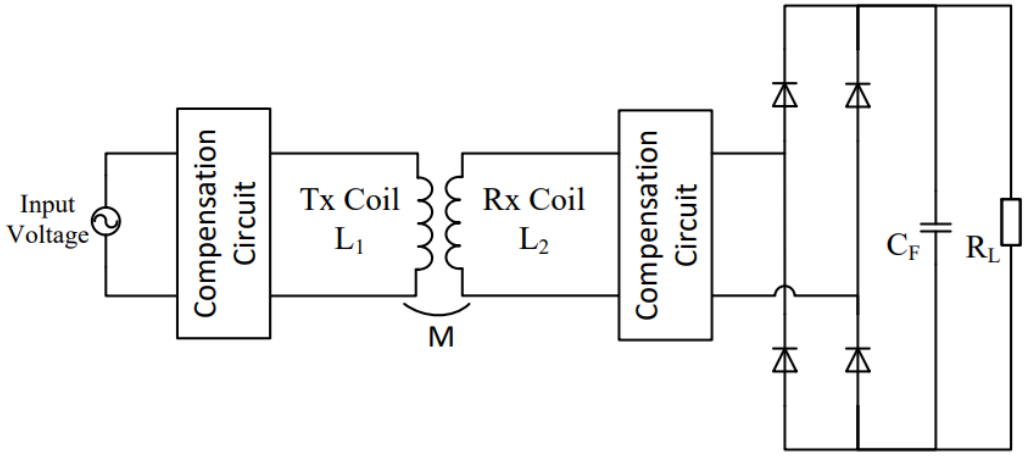

Fig 1.1 A conventional wireless power transfer (WPT) system

1.1.2. Applications of WPT

An important use of wireless power transfer (WPT) is demonstrated in Fig. 1.2, namely in the context of electric vehicles (EV). Given the phenomenon of climate change, there is a general consensus that it is imperative to decrease the release of greenhouse gases and transition towards the utilization of renewable energy sources. Therefore, Given the worldwide shift towards renewable energy sources, electric vehicles (EVs) are positioned to decrease our reliance on petroleum and facilitate the utilization of domestically sourced and renewable electricity. Several governments have provided incentives to electric vehicles (EVs), leading to a significant increase in EV sales in recent years. According to projections, the number of electric vehicles (EV) on the road worldwide is expected to reach 20 million by 2020 [2]. Nevertheless, electric cars (EVs) still fall short in terms of driving range and charging time when compared to traditional gasoline vehicles. Manufacturers have been compelled to enlarge the battery size due to the restricted driving range. Tesla's EV Model S P100D, which holds the title for being the

production EV with the longest range in the world, can surpass 300 miles on a single charge. On the other hand, this long range comes at a price: the 100-kWh battery pack makes the EV very expensive at $134,500 [3]. Moreover, the Tesla supercharger, recognized as the swiftest charger globally, can deliver a range of 170 miles within a 30-minute charging session [4]. However, this falls significantly short when compared to the mere minutes required for recharging a traditional gasoline vehicle. By employing dynamic wireless power transfer (D-WPT), the aforementioned concerns can be alleviated by the wireless charging of electric vehicles (EVs) while they are in motion. This can enhance the EV's total driving distance, decrease the required battery capacity, and minimize the necessity for recharging.

Static wireless power transfer (WPT) can enhance dependability, usability, and safety by eliminating the need for users to physically connect and disconnect connectors. Additionally, the adoption of contactless technology allows for greater weatherproofing of charging points.

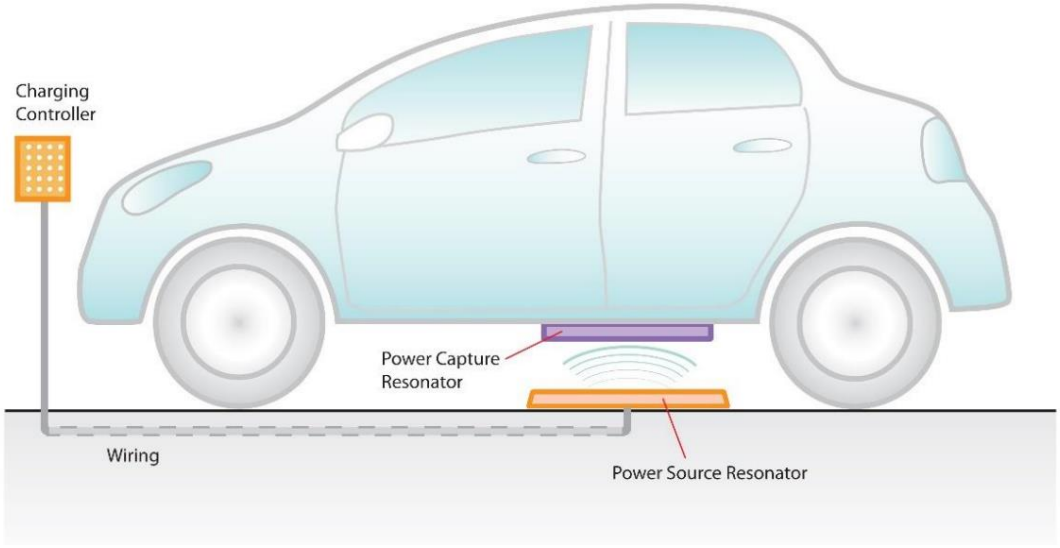

Fig 1.2 Wireless Power Transfer (WPT) for Electric Vehicles (EV) charging

Implantable biomedical devices offer another potential application for wireless power transfer (WPT). To suit operational needs, these devices are commonly placed inside the body (Fig.1.3). Historically, implanted batteries or percutaneous wires powered these gadgets. Current power distribution techniques limit implantable device functioning and put users at risk of infections owing to cables

or invasive battery replacement surgeries. Alternatively, transcutaneous power transmission can be accomplished through the use of WPT technology. WPT provides an inexhaustible energy supply for these biological implanted devices and changes the established standards of their operation. Traditional pacemakers require surgery to change the battery every 5 to 15 years, depending on the patient. This can be easily prevented by incorporating Wireless Power Transfer (WPT) technology [6]. The occurrence of infections caused by the wires used to transmit electricity to the implantable device or battery can also be minimized.

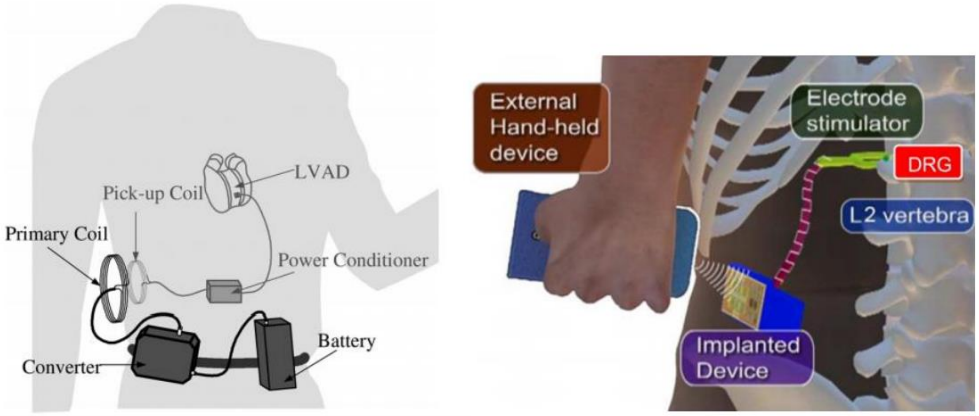

Fig 1.3 Biomedical devices that can be implanted into the body

Mobile consumer devices like phones are another challenging use case. Because to their widespread use, mobile phones now outnumber people [9]. However, the technical challenges of adopting wireless power transfer (WPT) in smartphones have hindered its adoption. High misalignment, large gap distances, small coil diameters, metallic phone housings, and excessive-powered charging are these challenges. The wired option, on the other hand, has undergone major advancements in terms of ease, particularly concerning the creation of bidirectional connectors such as USB type C, Apple's lightning connectors, and Qualcomm's QC3.0. When it comes to the rate at which electrical power is transferred, WPC Qi wireless fast charging permits a maximum of 15 W, which is the same as the QC2.0 wired standard that Qualcomm has developed [10]. The QC3.0 and USB type C wired protocols developed by Qualcomm, on the other hand, are capable of delivering power of up to 18 W [11] and 100 W [12] accordingly.

Consequently, the integration of the Wireless Power Transfer (WPT) technology into mobile phones has experienced a notable decline in pace in recent years. In order to increase traction, WPT must enhance its alignment, gap distance, and charging power.

Fig 1.4 Wireless Power Transfer (WPT) technology enables the simultaneous charging of several mobile devices.

1.2. Motivation

The utilization of WPT will further expand in tandem with the advancement of contemporary technology. Wireless Power Transfer (WPT) has the capacity to surpass the physical constraints of traditional cable power in the following domains:

- Operational versatility

  Wireless Power Transfer (WPT) has the advantage of being able to function in conditions that were previously not feasible due to the inflexibility of wired power systems. WPT technology enables the operation of a mobile robot in hard-to-reach areas and the charging of electric vehicles while they are moving. Wireless Power Transfer (WPT) technology would allow self-driving electric vehicles (EVs) to be charged automatically, eliminating the need for human involvement. This would result in the creation of a fully autonomous transportation solution.

- Convenience

  The wireless power transfer technology allows for effortless operation, eliminating the need for connected power. This enables the convenient charging of electric vehicles, implantable biomedical devices, mobile devices, and other similar gadgets. Such advancements have the potential to bring about a profound transformation in our daily lives.

- Protection

  Wireless Power Transfer (WPT) enables the transmission of electrical power without the need for physical connections. This mitigates the potential hazard of electric shock for the user. Wireless power transfer (WPT) ensures the safety of users of implantable biomedical devices by eliminating the risk of infections caused by charging cords or invasive battery replacement procedures.

- Isolation

  In addition to providing physical isolation by totally insulating the system from the environment, WPT also gives the benefit of electrical safety by providing electrical isolation between the transmitter (Tx) and receiver (Rx) sides.

- Designing with freedom

  Wireless charging technology enables the creation of creative designs that would be unattainable with traditional conventional conductors.

The aforementioned potentials have spurred Wireless Power Transfer (WPT) to become a highly attractive research area. While wireless charging has been used in various applications of different power levels, research is still ongoing to improve its performance. This includes the optimization of power transfer efficiency, the resolution of coil misalignment concerns, and the development of strategies to optimize coupling, among other factors. Furthermore, the D-WPT system makes it possible for wireless power transfer (WPT) to remain in place even when the receiver (Rx) is in motion. The system's functionality and adaptability are both significantly enhanced as a result of this. By way of illustration, electric vehicles are no longer required to be static in order to receive power wirelessly any longer. In spite of this, it is still possible to charge electric vehicles wirelessly by utilizing transmitters that are

positioned along the path of the vehicle through a process known as flexible wireless power transfer (WPT).

1.3. Objective and Scope

Within the scope of this thesis, the objective is to improve the total effectiveness of a wireless power transfer (WPT) system by employing a design technique for compensating circuits that are capable of adjusting to a variety of load conditions. Efficiency in power transfer, gap distance, and tolerance for misalignment are all included in the modifications. Furthermore, a control approach is proposed for the administration of WPT. This control method minimizes communication and WPT system complexity by controlling on the transmitting (Tx) side.

Contribution of the Thesis

The thesis addresses:

Chapter 1 This thesis provides an explanation as to why this study was carried out, as well as a description of the aims and objectives of this dissertation.

Chapter 2 examines the research regarding WPT systems in the literature. Static and dynamic WPT systems are the two types of WPT systems that are separated from one another. Other topics that are covered include the various kinds of compensating circuits that are utilized in WPT systems.

Chapter 3 explains, application-specific, the design principles and compensation circuits of WPT systems.

Chapter 4 presents a detailed explanation of a proposed three-phase wireless power transmission system with an active front-end rectifier. The system is designed specifically for battery charging applications.

Chapter 5 presents a Performance of wireless power transfer using a diode bridge rectifier, specifically designed for charging batteries. The simulation also takes into account the misalignment of the coils.

Chapter 6 evaluation of the Performance of a Three-phase Active Front End PWM Rectifier in the Configuration of an Air-Core Two-Coil WPT System and Investigating

Inductive Power Transfer Technology to Improve Electric Vehicle Charging Efficiency and Tolerance.

Chapter 7 Concludes the thesis and suggests potential avenues for future research that can be further investigated.

Chapter 2

Literature Review

There are many different kinds of WPT systems, including static WPT systems and dynamic WPT systems, and the purpose of this chapter is to provide a comprehensive literature review on it. The development of WPT is being driven by a variety of applications, including but not limited to electric vehicles, biomedical implants, and consumer electronics, the like. In addition, WPT compensation circuits are discussed quite briefly. In conclusion, a discussion is held regarding the performance indices for the WPT system.

2.1 Description of Wireless Power Transfer (WPT) Systems

The technique known as wireless power transfer (WPT) makes it possible to transmit electrical energy without the requirement for any physical connections first being established. A number of different techniques, Wireless power transfer can use RF waves, microwaves, lasers, capacitive coupling, and magnetic resonance, inductive coupling. Although capacitive coupling is an exception, most of these technologies rely on electromagnetic wave principles. However, they vary in terms of their operation principles and methods. In general, these technologies can be classified into two main categories based on their transmission range: near field and far field. RF waves, microwaves, and lasers are classified as far-field wireless power transmission (WPT) methods because they often operate over distances that are much greater than the wavelength of their electromagnetic waves. These technologies have the capability to transmit power without the need for wires over distances of tens of thousands of kilometres. This is achieved by transferring power from solar satellites to ground rectenna. The wavelengths used in these technologies are very short, with operational frequencies ranging from megahertz to gigahertz. Nevertheless, the far field wireless power transfer (WPT) methods encounter low efficiency and exhibit directionality, necessitating accurate alignment for successful power transmission. Near field wireless power transfer (WPT) methods

are also known as inductive coupling, capacitive coupling, and magnetic resonance coupling. This is due to the fact that these methods function at shorter distances in comparison to the wavelengths that are utilized. On the other hand, methods of near field wireless power transfer (WPT) do not necessitate precise alignment and are capable of transmitting enormous volumes of power while maintaining a high level of efficiency. However, the effectiveness of the near field wireless power transfer (WPT) methods declines quickly as the distance of transfer increases. A wireless power transfer (WPT) system that relies on inductive coupling must employ high-frequency electric currents to excite the Tx's main coil. The frequency range between 10 kilohertz and megahertz is the operational frequency [24]. An electromagnetic field is generated by the high-frequency electric current that is transmitted from the transmitter (Tx) to the receiver (Rx) or secondary coil. This electromagnetic field inductively links with the receiver, which enables power transmission. Due to the fact that the induced impedances of the primary and secondary coils are large, this technique is considered to be uncompensated. Due to the high frequency of operation, there are large magnetic impedances at both the input and output of the WPT system [25].

Both main and secondary coils feature compensating capacitors to lower impedances. By adding externally lumped capacitors [26], the magnetic resonance method changes the inductive and capacitive impedances of both fields. Operating the WPT system at its resonance frequency improves power transfer, efficiency, and transfer gap compared to uncompensated inductive coupling [14]. One can also use parasitic coil capacitance to correct coil inductance. The coil parasitic capacitance-dependent operating frequency must be substantially higher to reach the coil self-resonance frequency [27], [28].

2.1.1 Static WPT system

Conventional wireless power transfer (WPT) systems don't move the electricity loads while power is being sent. Electric vehicles (EVs) [29–31], biomedical implants [32–35], consumer electronics [36–43], and other related items are included in the loads. You can use electromagnetic pairing between two or more electromagnetic couplers (or coils) to send power remotely through a separation

gap. The way that inductive coupled wireless power transfer (WPT) works is shown in Fig. 2.1.In this setup, the transmitter coil carries a high-frequency electric current, which generates a magnetic field (B). The transmitter coil generates a magnetic field (B) that interacts with the receiver, which is separated by a distance of z [44]. The transmitter coil generates an electromagnetic field that causes an electric current to be created in the reception coil. Through the use of electromagnetic coupling, the wireless power transfer (WPT) system can transmit power ranging from microwatts to kilowatts with efficiencies above 90% [45]–[47]. The inductive coupled wireless power transfer (WPT) technology is resistant to dust, grime, water, and damage, unlike cables and connectors that can be affected by their surroundings.

EV charging is a promising application of static wireless power transfer (WPT). By utilizing static wireless power transfer (WPT) systems, it is possible to replace the charging cables and connectors, resulting in a significant reduction in running expenses associated with maintenance, theft, and other factors. A stationary wireless power transfer (WPT) system can charge Autonomous Vehicles (AVs) without human intervention. Despite its benefits, static wireless power transfer (WPT) fails to solve electric vehicle (EV) operating range and charges slower. Additional solutions include Dynamic Wireless Power Transfer (D-WPT) systems.

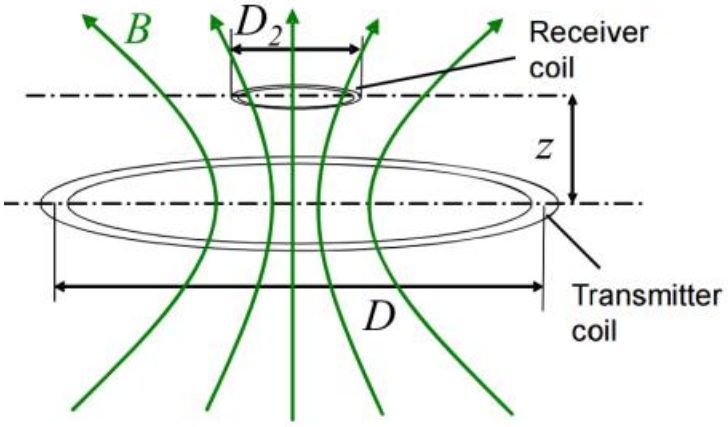

Fig 2.1 Inductively Coupled WPT system

2.1.2 Dynamic WPT system

A D-WPT system has electrical loads that can move and are in motion while the electricity is being sent. For instance, this would let electric vehicles (EVs), biomedical monitors that can be swallowed, and consumer electronics keep getting power while they're moving. Implementing D-WPT infrastructure in EVs enables the possibility of 'opportunistic charging' while the vehicles are in motion. This would effectively mitigate the issue of 'distance anxiety' experienced by numerous electric vehicle (EV) owners and substantially enhance the driving range of EVs beyond current battery capacities. 'Opportunistic charging' also decreases the required charging time for the electric vehicle through the static wireless power transfer technology, if needed. D-WPT systems can be broadly classified into two categories: Coils that are based on tracks and segments. The track-based D-WPT system has one long transmitter track that links to a receiver track that is much shorter. UC Berkeley and the Korea Advanced Institute of Science and Technology (KAIST) are two well-known places that use track-based D-WPT systems. KAIST has successfully showcased a track-based wireless power transfer (D-WPT) system using the online electric vehicle (OLEV).

It took 20 cm for this system to send 20 kW of power over that distance, and it did it 83% of the time. It was possible to send power because the emitter rails create a Shaped Magnetic Field in Resonance (SMFIR). The rails are between 5 and 60 meters long, and the pickup section is 80 cm long [48]. This results in drastically reduced coupling levels and a minimal distance between the transmitter and pickup modules, known as the relative transfer gap. The existence of large transmitter rails significantly contributes to both the challenges of electromagnetic interference/electromagnetic compatibility and the undesired exposure of humans to magnetic fields. The segmented coil-based D-WPT system, on the other hand, uses a group of transmitter coils that are linked to high frequency power sources, as shown in Figure 2.2. Oakridge National Laboratory (ORNL) showed that they could efficiently send 2 kW of electricity over a 10 cm distance using 33 cm-diameter coils. The device had a maximum efficiency of 85% [54].

The implementation of a segmented coil-based D-WPT system presents extra hurdles, Even though it can fix the connection and electromagnetic interference (EMI/EMC) issues that the track-based D-WPT system. Segmented coil-based systems in D-WPT are susceptible to the relative movement of the coils. The interaction between the electromagnetic fields would be influenced, leading to changes in the efficiency and power levels that are transmitted. ORNL has demonstrated the efficacy of electrochemical capacitors in mitigating power fluctuations [51], aiming to eliminate power variations and enhance the stability of power flow. Furthermore, it is necessary to exert control over each individual coil segment to optimize the efficiency of the operation and ensure the absence of any undesired magnetic field when the movable load is not there. In accordance with the information provided in reference 55, segmented coils that are coupled to a single high frequency power source are provided with the capability to achieve automatic power distribution by making use of an auxiliary LCC adjustment. Utilizing the auxiliary circuit allows for the regulation of the current that is going through the coils. Because of this, there is no longer a need for any kind of external controller or sensor network.

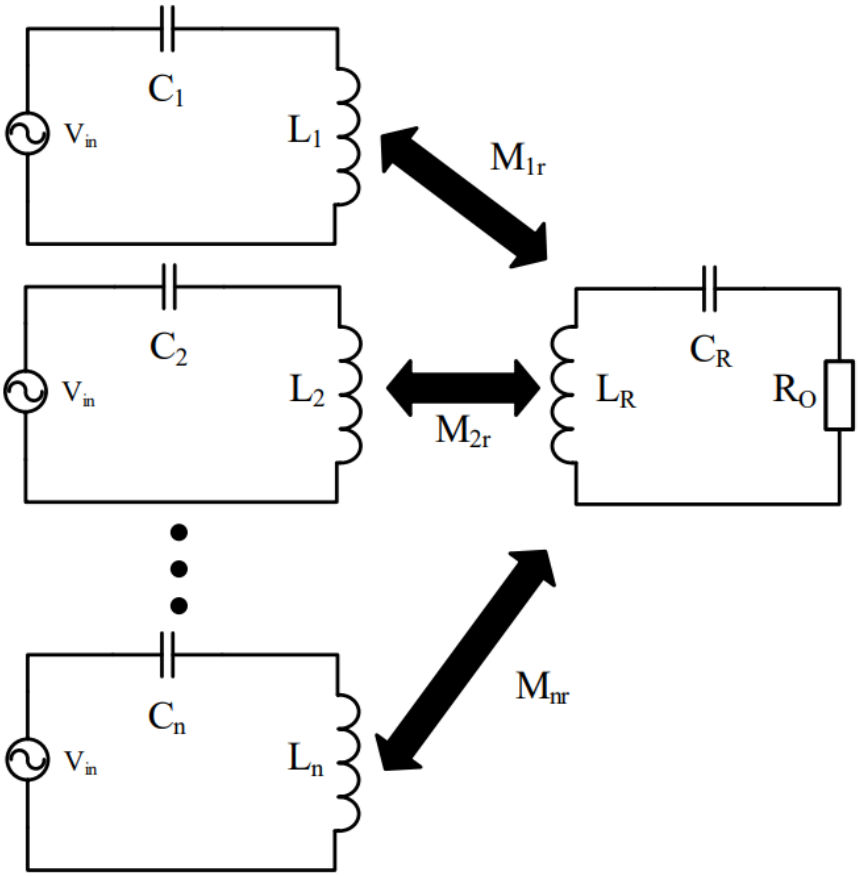

Fig. 2.2 A conventional D-WPT system

2.2 WPT Compensation Circuits

It is possible for WPT adjustment circuits to lower the VA rating of the WPT system, which raises the power transfer level and makes the system work more efficiently.Standard WPT compensation circuits make use of capacitors and are capable of being interconnected in a variety of configurations to cater to a wide range of requirements and standards. Fig. 2.3 to Fig. 2.6 displays the four distinct fundamental arrangements, specifically series-series (S-S), series-parallel (S-P), parallel-series (P-S), and parallel-parallel (P-P). The system input impedance equations can be determined using Kirchhoff's law, as shown in equations (2.1) - (2.8) [56].

Series-Series Compensation circuit:

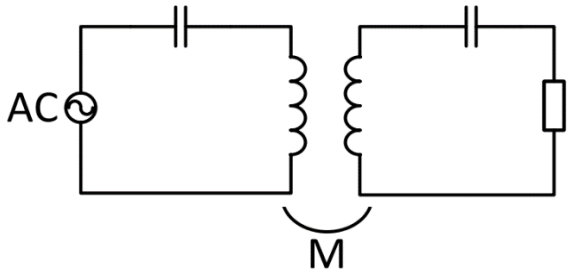

Fig.2.3 S-S compensation

$$Z_{in} = Z_{C1} + Z_{L1} + \frac{(\omega M)^2}{Z_{C2}+Z_{L2}+Z_L} \quad (2.1)$$

$$Z_{in} \approx \frac{(\omega M)^2}{Z_L} \quad (2.2)$$

Parallel-Series Compensation Circuit:

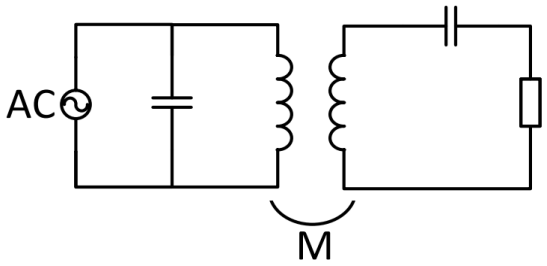

Fig.2.4 P-S compensation

$$Z_{in} = Z_{C1} + \frac{Z_{C2}^2(Z_S+Z_L)}{Z_P(Z_S+Z_L)+(\omega M)^2} \quad (2.3)$$

$$Z_{in} \approx Z_{C1} - \frac{Z_{C2}^2 Z_L}{(\omega_0 M)^2} \quad (2.4)$$

Series-Parallel Compensation circuit:

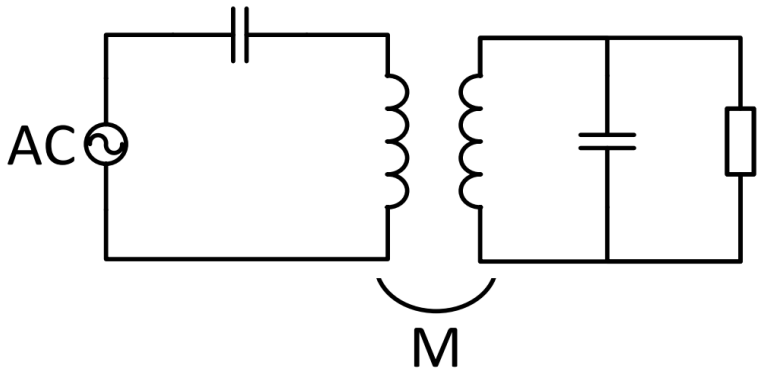

Fig.2.5 S-P compensation

$$Z_{in} = Z_P + \frac{(Z_{C2}+Z_L)\omega M^2}{Z_s(Z_{C2}+Z_L)-Z_{C2}^2} \quad (2.5)$$

$$Z_{in} \approx k^2(Z_{C2} + Z_L) \quad (2.6)$$

Parallel-Parallel compensation circuit:

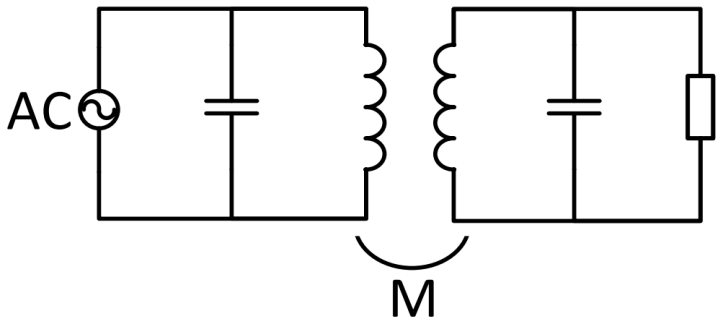

Fig.2.6 P-P compensation

$$Z_{in} = Z_{C1} - \frac{Z_{C1}^2[Z_S(Z_{C2}+Z_L)-Z_{C2}^2]}{Z_P[Z_S(Z_{C2}+Z_L)-Z_{C2}^2]+(\omega M)^2(Z_{C2}+Z_L)} \quad (2.7)$$

$$Z_{in} \approx Z_{C1} + \frac{Z_{C1}^2 Z_{C2}^2}{(\omega_0 M)^2(Z_{C2}+Z_L)} \quad (2.8)$$

People usually choose these basic compensation circuits because they are easy to understand and can work with a range of sources and loads. For example, voltage

sources with low input impedances (as shown in equations (2.1) and (2.5)) can be used in WPT systems with series transmission compensation circuits (S-S and S-P). On the other hand, equations (2.3) and (2.7) show that parallel transmission correction circuits can work with current sources that have high input impedances. It is best to use series compensation circuits for loads that have higher power (lower load resistances) and parallel compensation circuits for loads that have lower power (higher load resistances). This is because series compensation circuits are designed to compensate for higher power loads. It's important to note that the S-S compensation circuit is the only one whose resonance frequency stays the same no matter what the coupling and load conditions are. In spite of this, there is a very high voltage between the adjusting capacitors that are connected in series. Therefore, in high powered applications like electric vehicles and transportation, parallel compensation circuits are preferred due to their ability to limit current. This preference is supported by references [56] and [57].

2.2.1 Other Compensation Circuits

It is advised that alternate compensation circuits be utilized in addition to the fundamental compensation circuits in order to improve the overall performance of the WPT system. A parallel capacitor and a serial inductor are the components that make up the LCL compensation circuit, as shown in Figure 2.7 (a). It is a widely held belief that the LCL has a negative impact on VA ratings. The major goal is to improve the system's power and efficiency levels as much as possible. In addition, it is essential for the system to be able to act as a source of current while it is functioning at its resonance frequency [58–60]. The WPT system can control the flow of power because of this behaviour. It can change the emitter current by using a current source or a current source. Because it works better, the CLCL compensation circuit is used with the LCL compensation circuit. This circuit, shown in Fig. 2.7(b), lowers the amount of distortion in the input current [61]. The negative impacts of higher switching losses and decreased efficiency in the LCL adjusted WPT system are mitigated as a result of this action [62]. In spite of this, the regulation of the high-order CLCL compensated wireless power transfer (WPT) system is a complicated and expensive process. A significant reduction in the influence of the loading effect brought about by the S-S

compensation circuit is achieved by the utilization of the load transformation compensation circuit, which is illustrated in Figure 2.7 (c). Although the load transformation compensation circuit is more efficient than the S-S compensation circuit when applied to greater loads [35], the incorporation of an additional inductor would result in an increase in the required space, and the parasitic resistance of the inductor would have an effect on the efficiency of the circuit. As a result, the design and configuration of the load transformation compensation circuit must primarily be determined by the particular application and the operational conditions of the application. Through the incorporation of an extra capacitor, the LCC compensation circuit makes the LCL compensation circuit work better with harmonics, which leads to a power factor of one. The picture that shows this is Fig. 2.7(d) [29]. The LCC compensation circuit keeps the current source powers of the LCL compensation circuit.

This means the high-frequency power supply can manage transmitter coil current regardless of coupling and load. This simplifies transmitter power regulation, which benefits D-WPT systems. Coupling and load conditions differ in these systems [18], [55], [63]. In standby, when the receiver is far from the transmitter, the transmitter coil's constant current causes efficiency and EMI issues

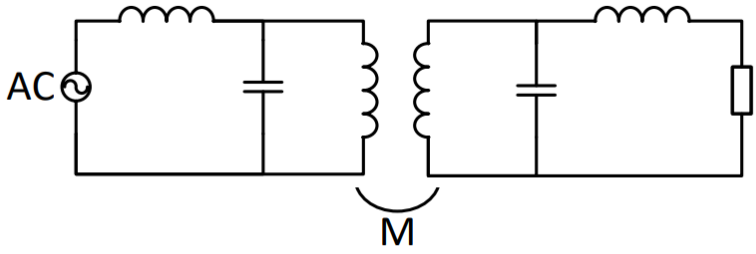

(a) LCL

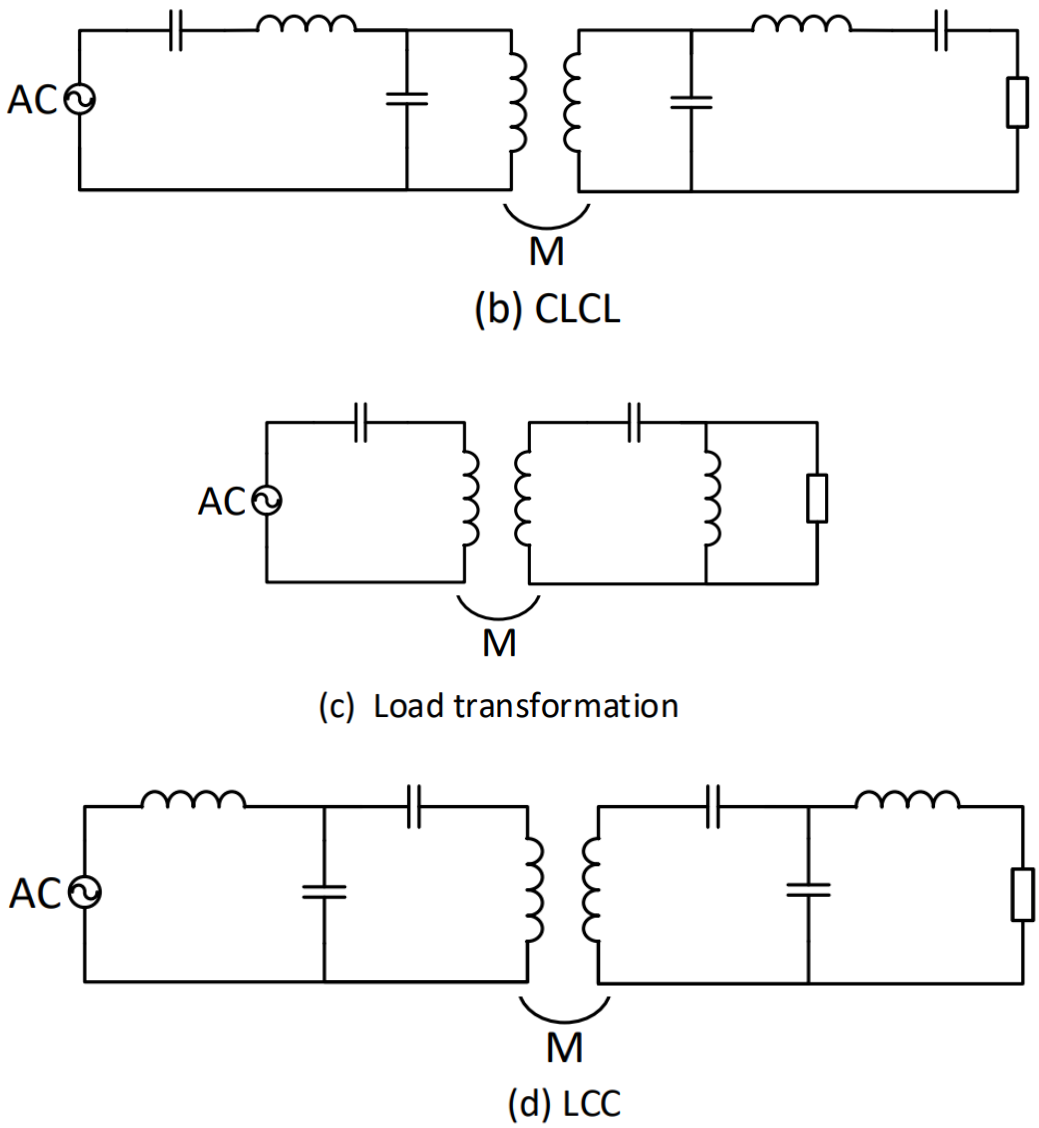

Fig. 2.7 WPT system with other compensation circuits: (a) LCL, (b) CLCL, (c) Load transformation and (d) LCC

2.3 Circuit Analysis

It is possible to conduct circuit analysis using a straightforward and precise modelling approach in order to assess the corresponding compensated WPT systems. In addition to helping with optimization and component selection, the circuit analysis would provide quantitative system performance indexes. Fig. 2.8 depicts the fundamental S-S compensated WPT system that is driven by an AC source operating at high frequencies. Power amplifiers (PAs) or inverters (PECs) are two examples of high-

frequency AC sources. The mutual inductance of M allows for the wireless transmission of electricity by coupling the transmitter and reception coils together. On the flip side, a circuit for charging batteries can be linked to the receiver coil and its compensating circuit. With respect to the state-of-charge (SoC) of the battery, the resistive AC load, RL, can be considered as an approximation of the charging circuitry load.

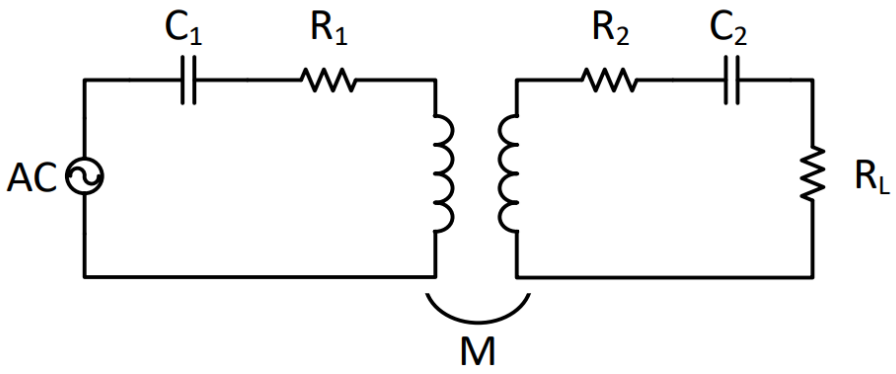

Fig. 2.8 Series-series compensated WPT system

As seen in Fig. 2.9 a two-port network equivalent circuit can be used to mimic the leakages and mutual inductances in loosely linked WPT systems. You may see the S-S compensated WPT system's circuit equations here:

$$\begin{bmatrix} V_{in} \\ 0 \end{bmatrix} = \begin{bmatrix} Z_{C1} + Z_{L1} + R_1 & j\omega M \\ j\omega M & Z_{C2} + Z_{L2} + R_2 + R_L \end{bmatrix} \begin{bmatrix} i_T \\ i_R \end{bmatrix} \quad (2.9)$$

2.3.1 Performance Indices

Wireless power transfer (WPT) system performance indices can be calculated using the two-port network equivalent circuit. WPT performance is measured by power transfer efficiency (PTE) and transmitted power. Fig. 2.9 shows the S-S compensated wireless power transfer (WPT) system's PTE:

$$PTE = \frac{|i_R|^2 R_L}{|i_T|^2 R_1 + |i_R|^2 (R_2 + R_L)} \quad (2.10)$$

Next, TP will explain the procedure that is used to normalize the output power of the WPT system with its input voltage, which is denoted by v_{in}. With regard to the S-S compensated WPT system, the following is a definition of the TP:

$$P_{out} = |i_R|^2 R_L \quad (2.11)$$

$$TP = \frac{P_{out}}{v_{in}^2} \qquad (2.12)$$

By means of the lumped components, coupling coefficient, and loading resistance, the performance indices enable WPT system optimization.

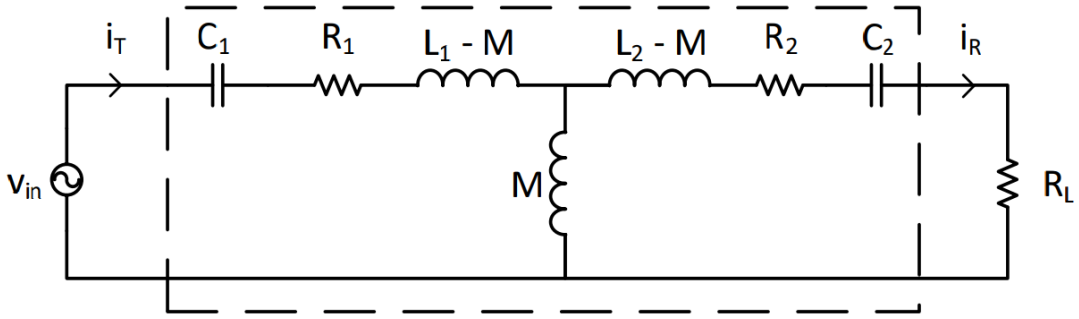

Fig. 2.9 The circuit model representing a wireless power transfer (WPT) system with series-series compensation and accounting for leakage inductances.

Chapter 3

COMPENSATION CIRCUITS FOR WPT

The compensating circuits used by WPT systems are diverse. In different environments, these compensatory circuits work differently. In this chapter, we use induced and reflected load equivalent circuits to find the operation frequency of the compensation circuits that maximizes efficiency. In the next part, we will conduct an in-depth analysis of the efficiency of the basic compensation circuits (series-series, series-parallel, and series-LCL) in relation to load variation, making use of the ideal frequency. The inclusion of crossover resistance, the load resistance points at where the efficiencies of the individual circuits meet, enhances the efficiency study. These circuits are further distinguished by resonant frequency response analysis. This chapter presents the theoretical analysis that is used to develop the efficiency-oriented design flow chart. Then, a few circuits are examined for voltage gain, transconductance, and transferred power. Finally, the results of the series-LCL and series-series experiments corroborate the given analysis, this illustrates a voltage gain and a constant transconductance, and it also indicates that the efficiency of the device is dependent on the equivalent load resistance. As load resistances increase, the difference in efficiency between the two compensation circuits may become more pronounced, reaching a high of 28% at a resistance of 500 Ω during the process.

2.1 Introduction

The WPT system relies on the Tx and Rx coils, which are its most important parts. These two coils are able to wirelessly transmit electrical power due to their mutual inductance (M). Adding compensating reactive components to both sides optimize and increases the power transfer. A typical WPT setup is shown in Fig. 3.1. For building the Tx side, you need a high-frequency AC source, a balancing circuit, and the Tx coil. On the Rx side of the circuit are the load, the rectifier, the adjusting circuit, and the Rx coil. To regulate the Tx current [65] or maximize power transfer [75], more complicated circuits have been employed; however, most WPT designs use basic circuits like series or parallel compensations. The load resistance (RL), which might

change, determines the RO, or equivalent output resistance, of the coils and compensation circuits. Charging batteries, driving motors, and dynamic WPT systems with numerous loads are all real-world instances of load variation. This variance will impact the overall performance and efficiency of the circuit, depending on the compensating circuit utilized.

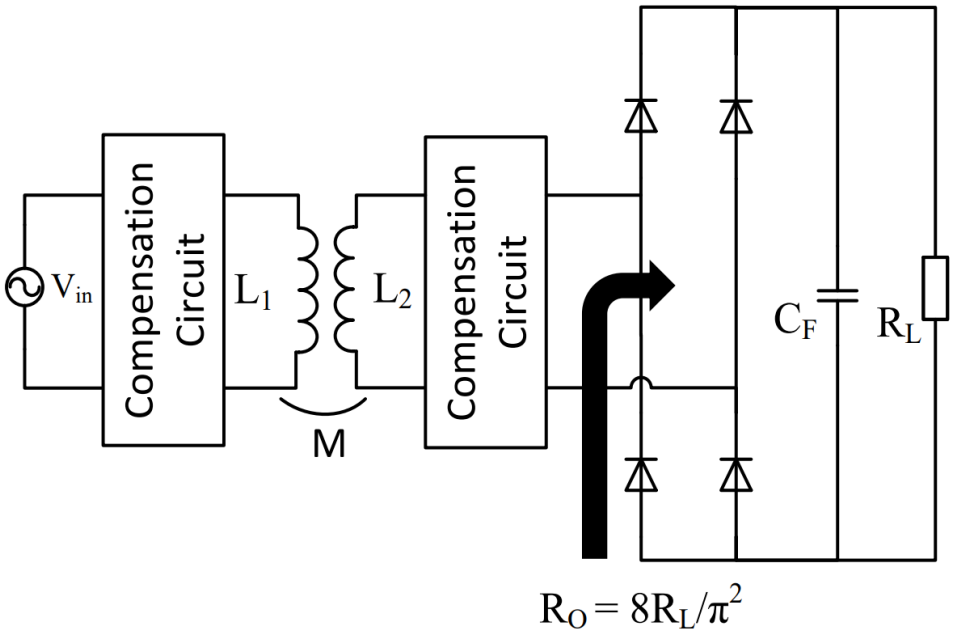

Fig. 3.1 Typical WPT system

Consequently, the chapter examines the series-parallel (S-P), series-LCL (S-LCL), and series-series (S-S) compensation circuits to find the ideal operating frequency for each type of efficiency. With the use of this frequency, which has been optimized for efficiency, we will investigate the ideal efficiency range in relation to the corresponding output resistance. Furthermore, differentiating the system can be accomplished by doing an analysis of the response of the resonance frequencies of the system with regard to coupling. Systems that use front-end power electronic converters with soft switching rely on the resonance frequency response. The next step is to present the detailed design flow chart that was derived from the aforementioned analyses. There will be coverage of other noteworthy evaluations as well, including transferred power (TP), output current, and voltage gains. Finally, a 2-coil WPT system's efficiency vs output resistance characteristic is shown, and the experimental

findings confirm that the circuits can achieve uniform transconductance and voltage gains.

2.2 Optimum Operating frequency

The resonance frequencies of the Tx and Rx in a standard WPT system can differ. The overall analysis of the compensation circuits will be carried out using both reflected and induced source models [17,19], with an emphasis on the efficiency-optimized frequency in this section.

2.2.1 Series Receiving Compensation

It is the S-S compensation circuit that is qualified to receive compensation for its component series. A representation of the compensating circuit can be created by modelling the equivalent circuits for the reflected load and the induced source, as shown in Figure 3.2. The formulae for the reflected impedance are presented in the following format:

$$V_{in} = (Z_{1s} + Z_{refS})i_{1ss} \tag{3.1}$$

Where $Z_{1s} = Z_{C1s} + Z_{L1} + R_1$ and $Z_{refS} = \frac{(\omega M)^2}{(Z_{C2s}+Z_{L2}+R_2+R_0)}$

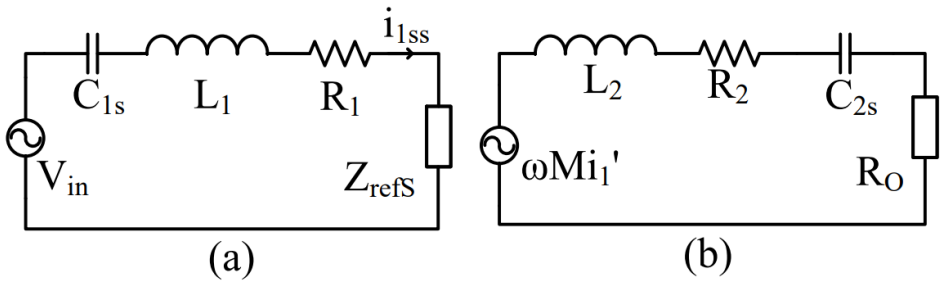

Fig.3.2 S-S compensation circuit: (a) Reflected impedance and (b) induced source models for S-S compensation circuit

It is feasible to treat R1 and the projected impedances of both circuits as being in series when evaluating efficiency. This is something that can be determined. The reason for this is that the reactive components, C1p and L1, do not require any actual power to function. For this reason, the only component of the reflected impedance that is taken into consideration in equation (3.1) is the real part. Through the utilization of the

comparable models of both compensation circuits, it is possible to illustrate the overall efficiency of the system:

$$\eta = \frac{\Re(Z_{refS})}{\Re(\boldsymbol{Z_{refS}})+\boldsymbol{R_1}} \times \frac{R_0}{R_0+R_2} \tag{3.2}$$

The primary focus of our interest lies in the compensation circuit, specifically on the component of reflected impedance, Z_{refS}. In order to optimize efficiency, it is necessary to maximize Z_{refS} and minimize R_1. To determine the maximum point of Z_{refS} with respect to frequency, a differential technique is applied. The differential equation is solved in order to determine the optimal frequency. In order to create an approximation, the terms with higher orders of C_{2s} ($C_{2s} << L_2 << R_2$) are neglected. The resulting approximation is shown below:

$$\omega_{SS-eff} = \frac{i\sqrt{2}}{\sqrt{C_{2s}^2R_2^2+2C_{2s}^2R_2R_0+C_{2s}^2R_0^2-2L_2C_{2s}}} \approx \frac{1}{\sqrt{L_2C_2}} \tag{3.3}$$

Based on equation (3.3), we can say that the frequency that works best for efficiency is the same as the resonance frequency of both the Rx coil and the S-S correction circuit.

2.2.2 Series Transmitting compensations (S-S, S-P and S-LCL)

The simplicity of the S-S compensating circuit is one of the reasons why it is so widely utilized. On both the transmitting and receiving sides of the circuit, the capacitors, which are represented by the letters C1 and C2, are linked in series with the coils that correspond to them. Assuming that the skin and proximity effects of the coils are taken into consideration in the respective coil resistances (R1 and R2) and that the coils are connected to one another, the following equations can be used to describe the circuit for this system:

$$V_{in} = i_{1ss}(Z_{C1s} + R_1 + Z_{L1}) - i_{2ss}(Z_M) \tag{3.4}$$

$$i_{ss}Z_M = i_{2ss}(Z_{L2} + R_2 + Z_{C2s} + R_0) \tag{3.5}$$

Where $Z_{C1s,C2s} = {}^{1}/_{(j\omega C_{1s,2s})}$, $Z_{L1,L2} = j\omega L_{1,2}$ *and* $Z_M = j\omega M$

During the study, the fundamental harmonic approximation (FHA) will be employed to streamline the analysis. The simplified current equations at resonance frequency are derived from equations (3.6) and (3.7).

$$i_{1ss} = \frac{R_2+R_0}{R_1R_2+R_1R_0+\lambda_1\lambda_2k^2}V_{in} \tag{3.6}$$

$$i_{2ss} = \frac{j\omega_0M}{R_1R_2+R_1R_0+\lambda_1\lambda_2k^2}V_{in} \tag{3.7}$$

Where coupling coefficient $k = {M}/{\sqrt{L_1L_2}}$, $\lambda_{1,2} = \sqrt{{L_{1,2}}/{C_{1s,2s}}}$

$$\omega_0 = {1}/{\sqrt{L_{1,2}C_{1s,2s}}} \tag{3.8}$$

The efficiency of the S-S compensating circuit is determined from equations (3.8) and (3.9).

$$\eta_{S-S} = \frac{\lambda_1\lambda_2R_0k^2}{(R_2+R_0)(\lambda_1\lambda_2k^2+R_1R_2+R_1R_0)} \tag{3.9}$$

Exhibits a nonlinear correlation with RO. By taking the derivative of equation (3.10) with respect to RO and utilizing coils of superior quality, the point of maximum efficiency is estimated to be:

$$R_{O(SS),\eta=max} = \frac{\sqrt{R_1R_2(\lambda_1\lambda_2k^2+R_1R_2)}}{R_1} \approx \sqrt{\lambda_1\lambda_2k^2} \tag{3.10}$$

According to research, WPT systems with S-S compensation work best at low load resistance. This is especially true for WPT systems that are loosely linked and have a coupling coefficient (k) of less than 0.2. It's also important to look at the load resistance at high efficiency along with the coupling coefficient.
The maximum value of $R_{O(SS),\eta=max}$ is also influenced by the ratio between the coil (Tx or Rx) and the compensating capacitance. This ratio can be modified as a design parameter for the WPT system in order to optimize its maximum value of $R_{O(SS)}$, which is denoted by the symbol η=max.

Table 3.1 Summary of circuit efficiency analysis

	$R_{O,\eta=,max}$	η_{approx}
S-S	$\frac{\sqrt{R_1R_2(\lambda_1\lambda_2k^2+R_1R_2)}}{R_1}$	$\frac{\lambda_1\lambda_2k^2}{\lambda_1\lambda_2k^2+R_1R_2+R_1R_0}$
S-P	$\frac{\lambda_2\sqrt{R_2(\lambda_1\lambda_2k^2+R_1R_1)(\lambda_2^2R_1+\lambda_1\lambda_2R_2k^2+R_1R}}{\lambda_1\lambda_2R_2k^2+R_1R_2^2}$	$\frac{\lambda_1\lambda_2^3k^2}{\lambda_1\lambda_2^3k^2+\frac{\lambda_2^4R_1+\lambda_1\lambda_2^3R_2k^2}{R_0}}$

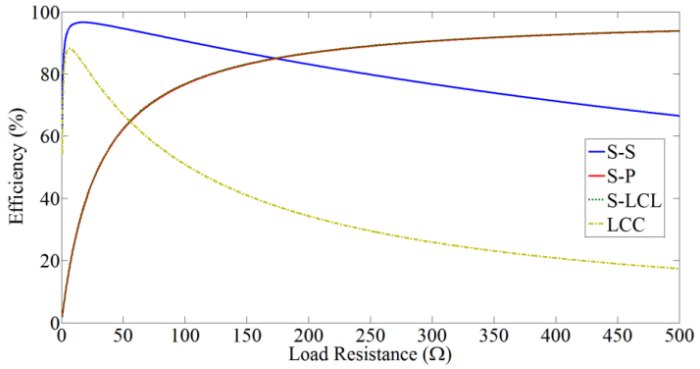

Fig 3.3 Load resistance efficiency for compensated S-S, S-P, S-LCL, and LCC WPT systems

Chapter 4

THREE PHASE WIRELESS POWER TRANSFER WITH ACTIVE FRONT END RECTIFIER

3.1 Introduction

During the preliminary stage of the wireless electric vehicle (EV) charger that is being proposed, an AC-DC converter is utilized to provide direct current (DC) power to the high-frequency (HF) inverter. A converter is integrated into the following component of the charging system under consideration, facilitating the conversion of Direct Current (DC) to High Frequency Alternating Current (HFAC). By facilitating the conversion of DC current to HFAC, this converter supplies the principal (Tx) coil with HFAC energy for the purpose of cordless power distribution. The wireless power transfer (WPT) system is constructed to employ Inductive Power Transfer (IPT), a widely recognized method for transmitting power over long distances between the transmitter (Tx) and receiver (Rx) coils without requiring a physical connection. The terminal module of the charger integrates an advanced capacitive filter mechanism with a wave diode converter to accomplish the primary goal of recharging the electric vehicles (EV) battery pack.

The Active Front End (AFE) rectifier is widely recognized within the power electronics industry for its remarkable efficiency in enabling the transmission of power in both directions. The seamless conversion of alternating current (AC) to direct current (DC) and vice versa is a characteristic that earns this device significant acclaim. The device exhibits outstanding power factor correction capabilities, which are evident in the load circuit's characteristics resembling those of a resistive load. Furthermore, it ensures that the voltage and current waveforms are in alignment. With an exceptional capacity for regeneration, it is capable of rerouting energy towards the initial power source, thus significantly improving energy efficiency. Furthermore, the introduction of the AFE rectifier greatly reduces the impact of harmonic distortions.

3.2 3-phase Active Front End Rectifier

Activity in Active Front-End (AFE) rectifiers has increased in tandem with the demand for high-power EV charging infrastructure. By operating in close proximity to the Unity Power Factor (UPF) and mitigating harmonic distortion, AFE rectifiers effectively restrict potential disruptions that may arise from the functioning of EV charging systems. They also provide exceptional dependability and efficiency. Component availability: as power levels increase, the variety of available components may become more limited and potentially more costly.

Consequences for the electrical grid: with the proliferation of rapid chargers, there is a corresponding escalation in harmonic distortion, leading to detrimental effects on sensitive equipment.

Due to the increased power consumption of rapid converters, their components are more susceptible to failure. Furthermore, in comparison to personal on-board chargers, commercial off-board chargers may undergo more frequent cycling, which could potentially shorten their operational longevity. As illustrate in Fig. 2. A three-phase AC power source provides the 415(V)-input power supply utilized by the AFE (Active Front End). The power source utilized for this purpose is frequently derived from a generator or the electrical utility. LCL filters diminish the magnitude of noise and harmonics. By means of a 6-switch Bridge rectifier, the transformation of alternating current (AC) voltage to pulsating direct current (DC) voltage is accomplished. The bridge configuration of power electronic switches, such as Insulated Gate Bipolar Transistors (IGBTs), is utilized in this rectifier. The function of the DC-link capacitor is to reduce ripple and stabilize the 800V DC voltage, which is characterised by its fluctuating nature.

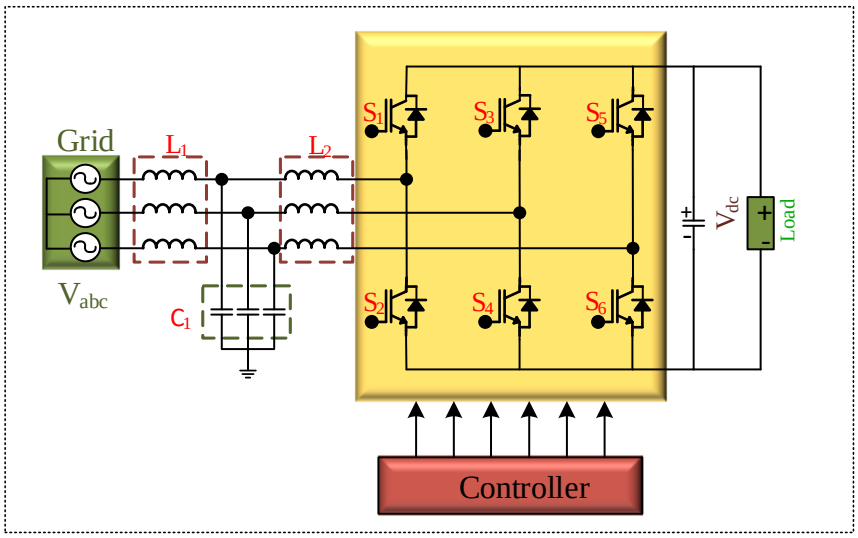

Fig.4.1. Circuit diagram of Active Front End Rectifier.

3.2.1 Control Methodology

SRFT Control theory [13], also known as d-q theory, is a framework that operates in the time domain. As shown in block diagram Fig.4.3, the three-phase abc component is converted to a two-phase component within the rotating reference frame. In addition to a rotation, the control algorithm integrates Park's transformation, which is an offshoot of Clark's transformation [12]. The evaluation of the direct and quadrature (d-q) components is conducted using Park's transformation.

The control methodology for adjustable speed drive systems and grid-connected converters can be applied identically due to their similarities. The literature describes three primary potential reference frame models that serve as the foundation for the control paradigm of these systems. The natural abc-reference frame, the stationary αβ-reference frame, and the synchronous dq-reference frame comprise these control structures. The orientations of the entities are visually represented in Fig. 4.2.

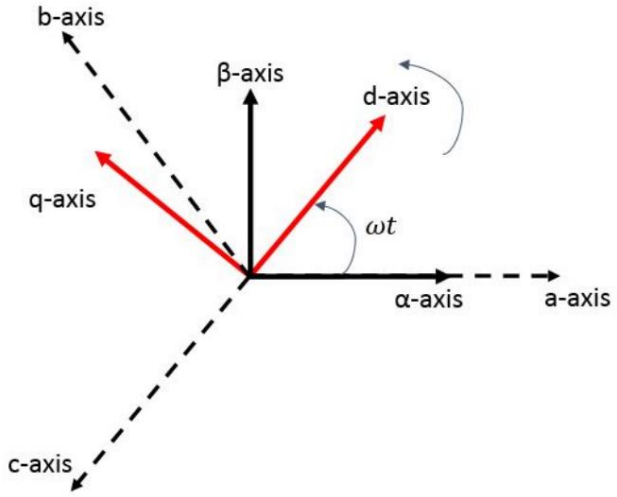

Fig. 4.2 The natural abc-reference frame, the stationary αβ-reference frame, and the synchronous d q-reference frame are oriented in this manner.

3.2.1.1 Synchronous d q-Reference Frame Control

In synchronization with a system quantity, the Park transformation, also known as the d q-transformation, converts a stationary system to a rotating orthogonal system. The process of transforming the stationary αβ-frame of into the d q-reference frame is illustrated in Eq. (4.1). [18]

$$\begin{bmatrix} d \\ q \\ 0 \end{bmatrix} = \begin{bmatrix} \cos(\omega t) & sin(\omega t) & 0 \\ -sin(\omega t) & cos(\omega t) & 0 \\ 0 & 0 & 1 \end{bmatrix} . \begin{bmatrix} \alpha \\ \beta \\ \gamma \end{bmatrix} \tag{4.1}$$

With the corresponding inverse transform of Eq. (4.2)

$$\begin{bmatrix} \alpha \\ \beta \\ \gamma \end{bmatrix} = \begin{bmatrix} \cos(\omega t) & -sin(\omega t) & 0 \\ sin(\omega t) & cos(\omega t) & 0 \\ 1 & 1 & 1 \end{bmatrix} . \begin{bmatrix} d \\ q \\ 0 \end{bmatrix} \tag{4.2}$$

Alternatively, the natural abc-reference frame can be transformed directly to the synchronous reference frame via Park transformation Eq. (4.3), [19].

$$\begin{bmatrix} d \\ q \\ 0 \end{bmatrix} = \frac{2}{3} \begin{bmatrix} \cos(\omega t) & cos(\omega t - 120) & cos(\omega t + 120) \\ -sin(\omega t) & -sin(\omega t - 120) & -sin(\omega t + 120) \\ \frac{1}{2} & \frac{1}{2} & \frac{1}{2} \end{bmatrix} . \begin{bmatrix} a \\ b \\ c \end{bmatrix} \tag{4.3}$$

With the inverse transform as indicated in Eq. (4.4).

$$\begin{bmatrix} a \\ b \\ c \end{bmatrix} = \begin{bmatrix} \cos(\omega t) & -sin(\omega t) & 1 \\ cos(\omega t - 120) & -sin(\omega t - 120) & 1 \\ cos(\omega t + 120) & -sin(\omega t + 120) & 1 \end{bmatrix} . \begin{bmatrix} d \\ q \\ 0 \end{bmatrix} \quad (4.4)$$

By employing synchronous reference frame (SRF) control, the d q-reference frame can be utilized; in this case, the d q-axis of Fig. 4.2 is synchronized with the grid-frequency as shown in Fig.4.3. Consequently, the fundamental frequency steady-state control variables of SRF controllers will be represented by DC values, in contrast to the stationary reference frame-based control systems which utilize sinusoidal quantities. This is a crucial characteristic of the SRF control, as the majority of stationary reference frame linear controllers that track AC components introduce significant stationary phase errors at fundamental and harmonic frequencies [20].

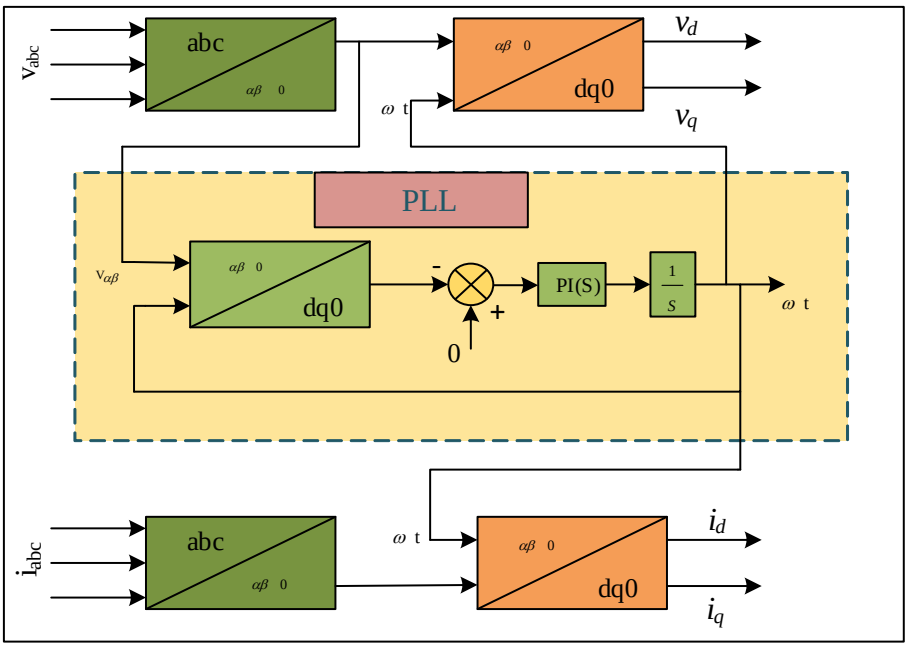

Fig.4.3 Block diagram of initial stage of control scheme.

3.2.1.1.1 Voltage loop control

As Fig.4.4 depicted that voltage-loop control refers to the process of regulating the DC-link voltage of a power converter, which is crucial for ensuring the converter operates correctly. The design of control systems frequently employs a Proportional-Integral (PI) controller in order to effectively regulate the DC-link voltage to its intended point of reference. By minimising voltage errors, this approach enhances

voltage stability in the presence of load fluctuations. The value of K_P & K_I for voltage control loop (Fig.4) are determined by the equation below.

$$T_{C1} = 220\mu s$$
$$C_1 = 100\mu F$$
$$K_P = \frac{3 * C_1}{T_{C1}} = 1.5$$
$$K_I = \frac{3 * (20 * 10^{-3})}{T_{C1}} = 300$$

3.2.1.1.2 Current loop control

The inner control loop is designed to control the active and reactive current components (i_d, i_q) within the grid's synchronous reference frame. In an ideal situation, the current of the converter should follow its reference value, which is adjusted by the outer voltage control loop. The determination of the values of K_P and K_I for the current control loop (Fig.4.4) is achieved through the use of the following equation.

$$T_{C1} = 220\mu s$$
$$C_1 = 100\mu F$$
$$K_P = \frac{3 * C_1}{T_{C1}} = 1.5$$
$$K_I = \frac{3 * (20 * 10^{-3})}{T_{C1}} = 300$$

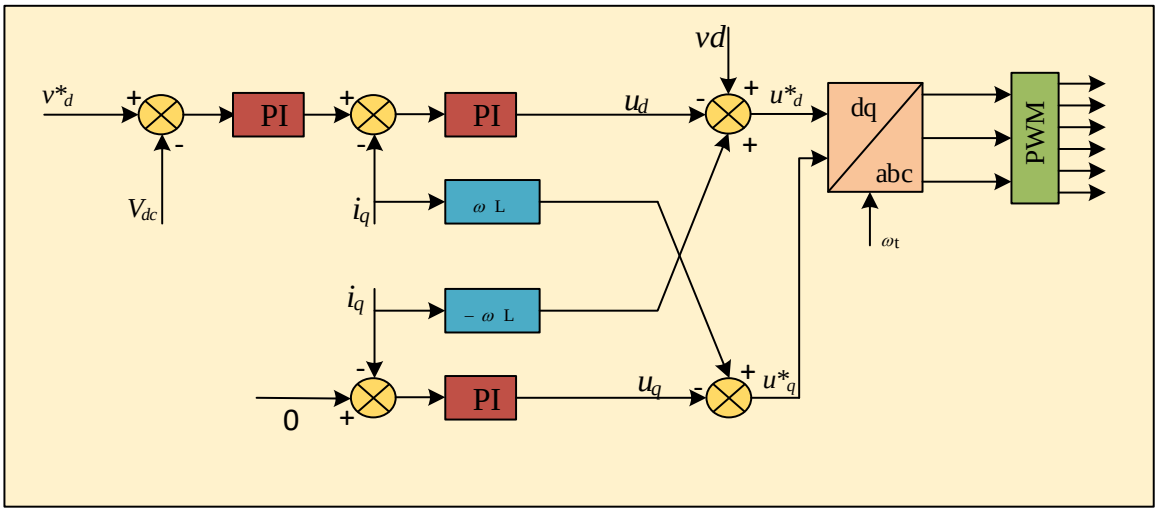

Fig.4.4 Voltage and Current loop Controlled Scheme

The activation of the voltage control loop of the AFE converter occurs when there is a modification in the voltage reference. The control loop functions by minimising the discrepancy between the actual voltage and the reference voltage, thereby aiming to sustain the output voltage at its desired magnitude as represented in Fig. 4.5.

In the represented Fig. 4.5, the reference voltage is augmented from 700V to 900V, the voltage control loop will detect an error between the reference voltage and the actual output voltage. The control loop, commonly employing a Proportional-Integral (PI) controller, is intended to drive the system towards augmenting the output voltage in order to align with the updated reference of 900V.

In a similar manner, when the reference voltage is diminished from 800V to 600V, the voltage control loop will instruct the system to correspondingly decrease the output voltage to the 600V.The parameters of the Active front end rectifier is in the table no.1 given below. The parameters of the AFE are in the table.4.1.

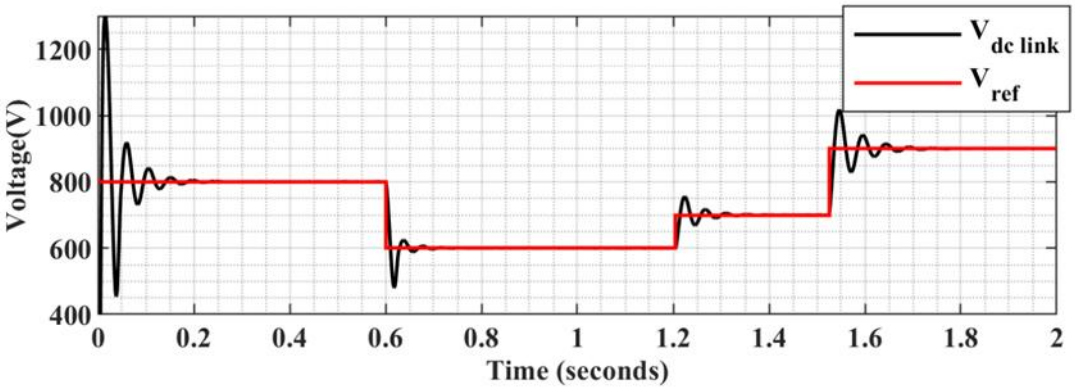

Fig.4.5 Output of AFE (V_{dc}) at different Voltage reference

Table.4.1 Active front End rectifier parameters

AFE Parameter	**Value**
Grid Voltage	415 V_{PP}
DC Link Voltage	800V
Grid Freq	50Hz
Switching Frequency	10kHz
Inductance (L_1 =L_2)	0.5mH
Capacitance(C_1)	100µF

3.3 Components of AFE Rectifiers

3.3.1 Power Semiconductor Selection

The majority of the AFE rectifier is made up of switches. The effectiveness of the AFE system as a whole depends on the dependability and efficiency of these switching elements. The performance of AFE rectifiers can be significantly enhanced by the introduction of new and enhanced devices, such as Wide Bandgap (WBG) semiconductor switches. The WBG devices can function at higher switching frequencies, block larger voltages, and tolerate higher junction temperatures. Furthermore, WBG devices have reduced conduction and switching losses. WBG active switches enable off-board chargers to run at even greater power levels while permitting increased power density within the weight and volume restrictions of the on-board charger. WBG chargers can have an efficiency of up to 98.5%.

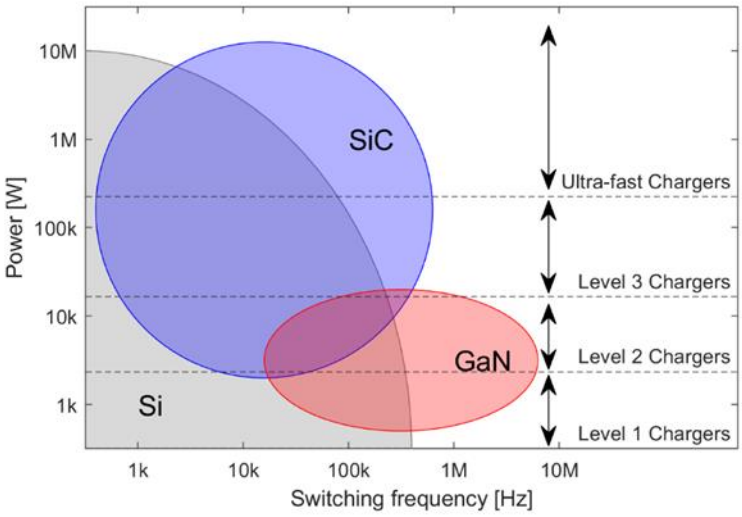

Fig.4.6 Application of power semiconductors by type.

3.3.2 DC Link Capacitor Selection

One of the key parts of power electronic converters is the DC link capacitor. Aluminium electrolytic capacitors metallized polypropylene film (MPPF) capacitors, and high-capacitance Multi-Layer Ceramic (MLC) capacitors are the three primary types of capacitors used in automotive applications. The highest energy density and capacitance are found in electrolytic capacitors, which are also more reasonably

priced. When it comes to fast charging applications, AFE DC link capacitors often have lower necessary capacitance values than single-phase charger capacitors. But these capacitors' current rating needs to match the rapid chargers' high-power rating.

3.3.3 Grid Side Filters Selection

For frequencies above resonant frequency, the third order LCL filter can attenuate by 60 dB per decade. It is made up of a parallel capacitor, a second series inductor on the grid side, and a series inductor on the inverter side. Furthermore, a dampening resistor is connected in series with the capacitor in order to reduce the resonance peak. An LCL filter can be used to obtain good attenuation across various load actions without being overly large or expensive. It is noteworthy that the grid side inductor in the LCL filter has lower harmonic current stress than the inverter-side inductor.

3.4 Active Front End Rectifier fed Air-Core Two-Coil WPT System

3.4.1 System Description

In this study, the proposed wireless electric vehicle (EV) charger as shown in Fig.4.6 encompasses four primary components, aimed at ensuring effective and dependable wireless power transmission. Beginning with the AC-DC Converter, it serves as the source of DC power and converts incoming Alternating Current (AC) into Direct Current (DC). The DC output is then channelled into a High-Frequency AC Inverter (HFAC), which transforms the DC into High Frequency Alternating Current (HFAC) for more efficient wireless power delivery. The subsequent stage consists of Wireless Power Transmission (WPT) utilizing Inductive Power Transfer (IPT) and involves a transmitting (T_X) and a receiving (R_X) coil. Powering the T_X coil with HFAC enables efficient energy transfer to the R_X coil in the EV via IPT, across the "air gap." Finally, the system incorporates a Full Wave Diode Rectifier, working in tandem with a Capacitive Filter, to convert the received HFAC back into DC. With the capacitive filter smoothing out irregularities, a consistent and refined DC output charges the EV battery.

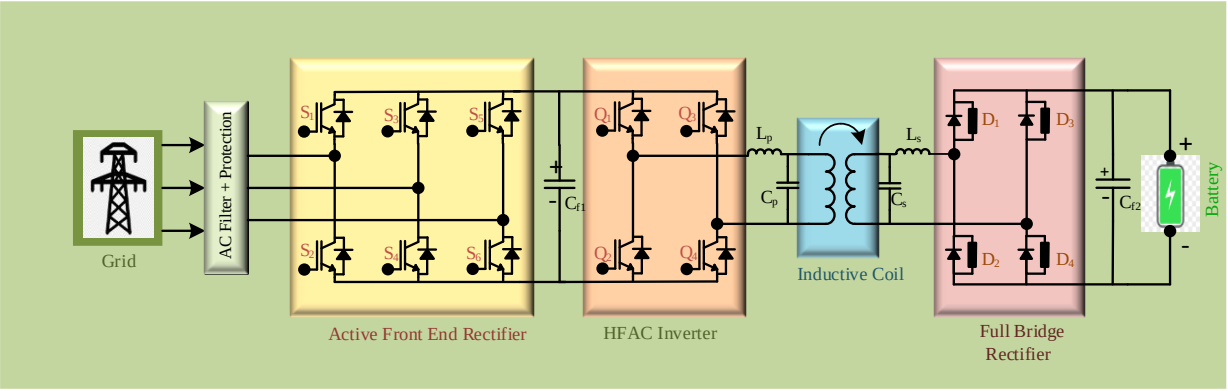

Fig.4.7 Electric vehicle charger topology with primary side charging station and secondary side charger circuit diagram

3.4.2 HFAC Inverter

The high-frequency alternating current (HFAC) inverter is configured with an open-loop control system [4]. It operates by switching at a frequency of 30kHz with a duty cycle of 50%. The input voltage, denoted as Vdc, is set at 800V.The inverter derives advantages from a decrease in size and weight, as well as enhanced response times. Despite the potential limitations in dynamic performance caused by the absence of feedback, the open-loop control system can still prove effective in a range of applications that prioritise stability and controlled conditions. The inverter produces an output of 800V AC voltage with a peak-to-peak amplitude, as illustrated in Fig.4.7.

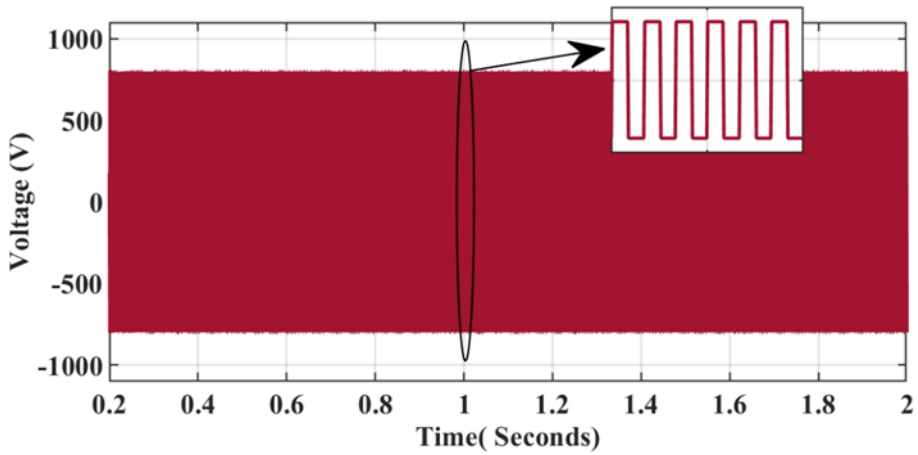

Fig.4.8 Output voltage of HFAC Inverter

3.4.3 Inductive Coil and Diode Bridge Rectifier

Wireless Charging Based on Inductive Power Transfer (IPT) [6]. IPT relies on the magnetic induction concept to deliver power without the use of a medium. It is based on Lenz's and Faraday's laws, according to which a conductor's time-varying current creates a magnetic field around it and a secondary loop's (receiver) time-varying magnetic flux generates voltage.

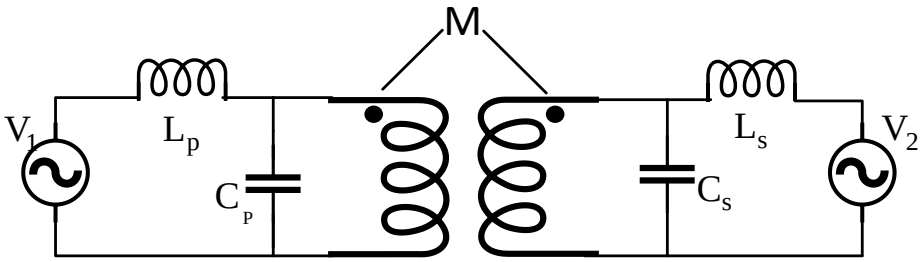

Fig.4.9 LC based multi-resonant Compensation.

According to the illustration in Fig.4.9, it can be observed that the 800V AC voltage, initially in the form of a square wave AC, undergoes compensation [7],[8] through an LC circuit (Fig.4.8), resulting in an output of 800V sinusoidal AC voltage. This compensated voltage is then supplied to the primary coil (v_p) and subsequently transmitted to the secondary coil, where it is transformed into a 1000V AC voltage (v_s), as depicted in Fig.4.10.

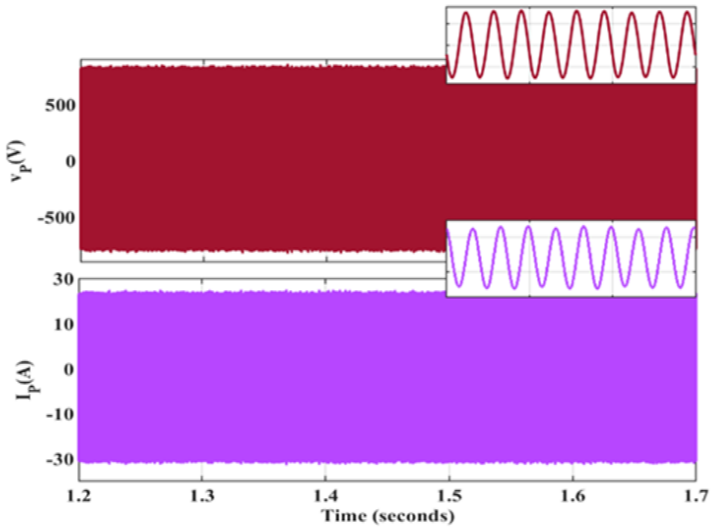

Fig.4.10 Voltage and current on the primary coil.

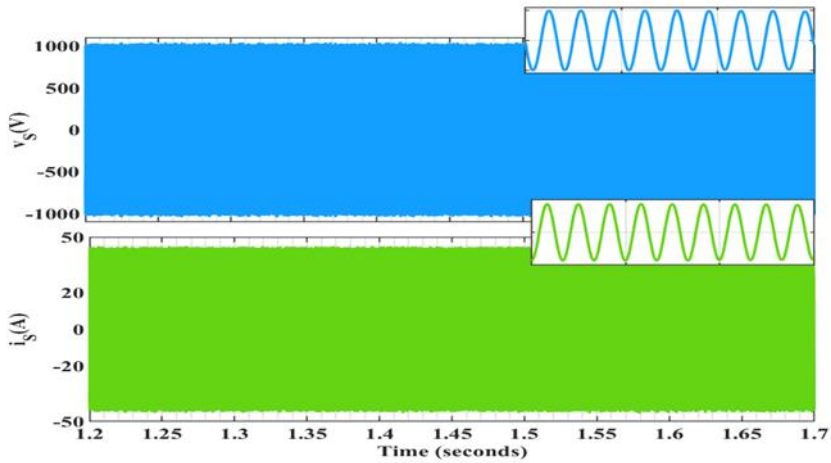

Fig.4.11 Voltage and current on the secondary coil.

Table.4.2 Inductive Coil parameters

Coil Parameter	**Value**
Roadside Winding Turns	$N_1 = 28$
Vehicle side Winding Turns	$N_2 = 28$
Diameter of Roadside Coil	$D_1 = 19cm$
Diameter of Vehicle side Coil	$D_2 = 19cm$
Self-Inductance of Roadside Coil	$L_{primary} = 155.243\mu H$
Self-Inductance of Vehicle side Coil	$L_{secondary} = 110.313\mu H$
Resistance of Roadside Coil	$R_1 = 0.23213\Omega$
Resistance of Vehicle side Coil	$R_2 = 0.20755\Omega$
Operating frequency	$f_s = 30kHz$

The Diode Bridge Rectifier with Capacitive Filter is a power electronic circuit utilised for the conversion of alternating current (AC) power to direct current (DC) power, with the added benefit of enhancing the quality of the output voltage waveform. The system comprises a complete bridge rectifier configuration incorporating four diodes to rectify the alternating current (AC) voltage. Subsequently, the rectified voltage is directed through a capacitive filter, thereby mitigating ripple, and yielding a more consistent direct current (DC) output voltage. The diode bridge rectifier is connected to the 48V lead-acid battery, which is being charged by its output as shown Fig.1of the proposed circuit diagram.

Chapter 5

SINGLE PHASE WIRELESS POWER TRANSFER WITH DIODE BRIDGE RECTIFIER

4.1 Introduction

The advancement and widespread usage of battery-powered devices are being impeded by a number of basic problems, including the low energy density, short lifespan, and high starting cost of electricity storage technologies [1]. The outstanding positional and mobile capabilities of inductive power transfer (IPT) technology have led to its proposal as a remedy to the unsolved problems associated with energy storage. This new technology has been under intense scrutiny from both the business and academic worlds. The device's battery life is significantly improved because it enables regular charging without a physical connection. A variety of battery-operated gadgets can have their energy storage limitations lifted with the help of modern wireless charging technology. It is possible to classify the uses of IPT technology as either low-power or high-power [2]. Things that fall under the high-power tier umbrella include power systems, electric vehicles (EVs), and manufacturing automation. In contrast, low-power level devices include things like consumer electronics, implanted medical devices, integrated circuits, and similar ones.

One of the main issues with conductive charging is the difficulty of handling high power wires while plugging in an electric vehicle (EV). Inappropriate handling or broken cables could cause hazards. Both theft and vandalism can occur with conductive charging techniques. Wireless power transfer, or WPT, was initially proposed in the 1800s by Nikola Tesla. It has developed into a competitive option and a practical substitute for cable charging systems over time. Instead of using the conventional plug-in interface, this technology allows for the transmission of electricity by electromagnetic or static waves, as shown in Fig. 5.1. This eliminates the need for physical contact. Wireless power transfer (WPT) systems rely on power

electronic converters to enable the transfer of power from the receiver to the drive system or batteries.

The WPT system possesses the following key features:

- The system can be categorized into various categories according to the transmit power ranges [5]. The WPT system functions within three distinct power ranges: low power, which is less than 1 kilowatt (kW); medium power, ranging from 1 to 100 kW; and high power, beyond 100 kW.
- The WPT system is capable of bidirectional (between the vehicle and the grid) and unidirectional (from the grid to the automobile) power transfer. Comparatively, the implementation of conductive charging via Vehicle-to-Grid (V2G) technology is more intricate than that of wireless charging. Vehicles can engage in vehicle-to-vehicle (V2V) charging both when they are moving and when they are stationary.
- Power can be transmitted over short distances, ranging from a few centimeters to kilometers, as well as over long distances.
- Power can be transferred using several types of media.
- The efficiency of the system depends on the medium employed for power transmission. Substantial losses have occurred in this area.

As an illustration, the author of the research asserted that an air-gap system, which uses air as the medium, exhibited a 5% greater efficiency compared to an underwater WPT system that uses water as the medium.

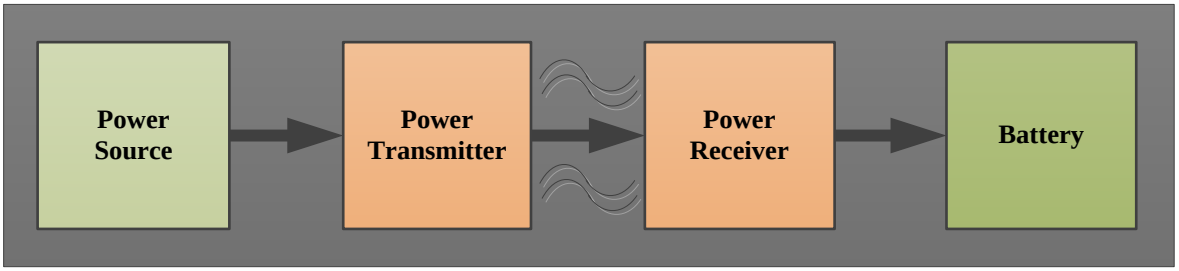

Fig.5.1 Basic Power flow diagram of Wireless Power Transfer

4.2 System Description

A wireless power transfer (WPT) system comprises three primary components: a high-frequency inverter, compensation networks, and magnetic couplers. The load in the EV charging application can be seen as having a uniform resistance at every level of output power. Fig.2 displays the circuit diagram of a typical Wireless Power Transfer (WPT) system, featuring a full-bridge inverter and a basic diode rectifier. The Fig.5.2 illustrates the self-inductances of the primary and secondary coils, denoted as L_p and L_s, respectively. The mutual coupling between the couplers is denoted by M. The coupling factor for the coils is defined as the ratio of M to the product of the inductance of the primary coil (L_p) and the inductance of the secondary coil (L_s). This coupling factor is represented by the symbol k. Furthermore, r_p and r_s represent the parasitic alternating current resistance of the coils [12]. The presence of AC resistance in the coils decreases their intrinsic quality factor, hence significantly impacting the theoretical efficiency of the system.

Increasing the distance between the coils increases the importance of improving the quality factor (Q) and coupling coefficient (k) in the architecture of both the primary and secondary coils for wireless power transfer (WPT) systems [11]. Ferromagnetic cores assist in directing flux, hence improving coupling, whereas losses occur due to ferrite core and coil ohmic losses caused by skin effect. Strategies such as employing Litz wire and maintaining flux density below saturation levels aid in reducing losses. Notwithstanding progress, the constraints of power and space pose substantial obstacles.

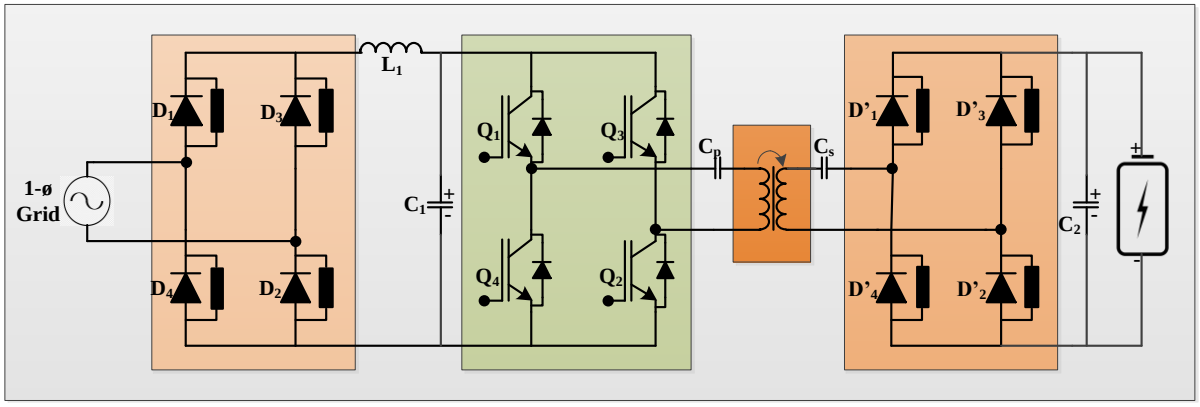

Fig.5.2 Proposed circuit of the wireless charging of Electric Vehicles

The operating frequency (ω), coil self-inductance (L), and coupling coefficient (k) are crucial factors that impact efficiency. Although the secondary coil voltage is theoretically capable of being increased at higher frequencies, the losses associated with such an increase are also higher [8]. The space available under the electric vehicle's chassis dictates the coil's maximum allowable dimensions. Nevertheless, the self-inductance of the coil can be enhanced by adding more turns to it. Coils of the same size, a larger diameter, and a shorter air gap are all ways to improve coupling [4]. Energy transfer efficiency, coil Q factor, size, and pairing coefficient are all crucial design parameters that must be carefully considered using the appropriate equations [5.2]-[5.10].

$$d_{xo} = d_{xi} + 2.[N.d_w + (N-1).\gamma] \tag{5.1}$$

This is where N stands for the number of turns in the coil, dw for the diameter of the wire, dxo for the diameter of the coil outside, and γ for the distance between successive turns.

$$k = \frac{M}{L_1.L_2} \tag{5.2}$$

The equation involves the following variables: M denotes the mutual inductance, S denotes the self-inductance of the secondary coil, L is the self-inductance of the main coil, and K denotes the coupling coefficient.

$$Q = \frac{\omega.L}{R} \tag{5.3}$$

where Q, τ, and R stand for coil inductance, resistance, and the quality factor, Hz, res pectively.

$$\eta_{max} = \frac{1}{1+\frac{2}{k^2Q_1Q_2}+\frac{2\sqrt{k^2Q_1Q_2+1}}{k^2Q_1Q_2}} \tag{5.4}$$

The value of η_{max} represents the highest energy transfer efficiency (%) and is determi ned by the connecting coefficient $\boldsymbol{k}$. The transmitting coil's quality factor is Q_1. A second quality indicator for the receiving coil is Q_2.

4.2.1 Series compensation

Both the primary and secondary compensation networks [9] in this design consist of a straightforward series capacitor, as seen in Fig.5.3. The impedance observed by the secondary coil, Z_{sec}, is represented in this circuit [15].

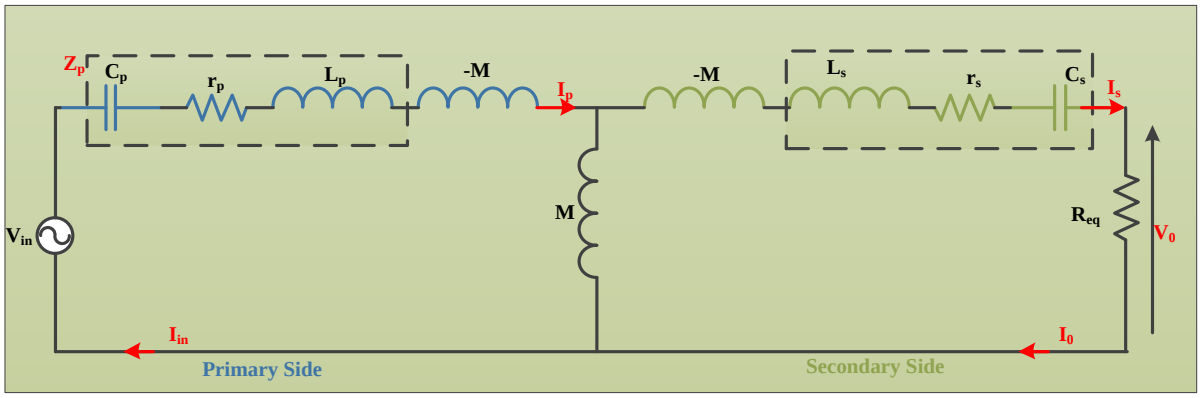

Fig.5.3 Resonant networks using series-series WPT technology

$$Z_s = Z_{sec} - \omega M j \tag{5.5}$$

where

$$Z_{sec} = R_{eq} + r_s + (L_s \omega - 1/\omega C_s) j \tag{5.6}$$

The inverter perceives the input impedance of the circuit as

$$Z_{in} = Z_r + Z_p = r_p + j (L_p \omega - 1/\omega C_P) + Z_r. \tag{5.7}$$

The input and primary- and secondary-side currents are determined based on the specified impedances of the circuit.

$$I_{in} = I_p = V_{in} Z_{in} \tag{5.8}$$

$$I_s = I_{in} j\omega M / (Z_s + j\omega M) = I_{in} j\omega M / Z_{sec} \tag{5.9}$$

Given that the output current (Io) is equivalent to the current flowing through the secondary-side coil, the output voltage can be mathematically represented as:

$$Vo = R_{eq} I_s = I_p j\omega M R_{eq} / Z_{sec} \tag{5.10}$$

4.2.2 Circular Coil simulation

The Circular coil's specifications were provided in Table 5.1. The Simulation model and magnetic field of the Circular coil [3] are shown in Fig.5.4 and 5.5, respectively [17].

Table.5.1 Specifications of Circular Coil

Name	**Value**	**Unit**	**Evaluated Value**	**Type**
mis_ang	0	deg	0	Design
Dist	10	Cm	10	Design
R_out	20	Cm	20	Design
R_in	10	Cm	10	Design
$Miss_{Xaxis}$	0	Deg	0	Design
Current	10	A	10	Design
N1	38		38	Post Processing
N2	38		38	Post Processing
H_miss	0	cm	0	Design
N2	38		38	Post Processing
H_miss	0	cm	0	Design

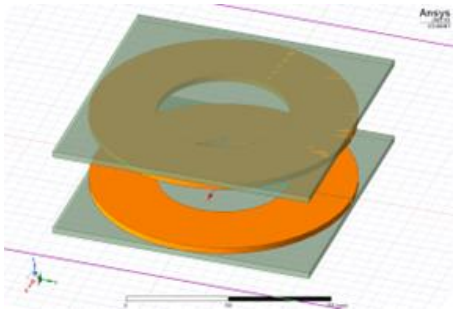

Fig.5.4 The simulation model of circular coils.

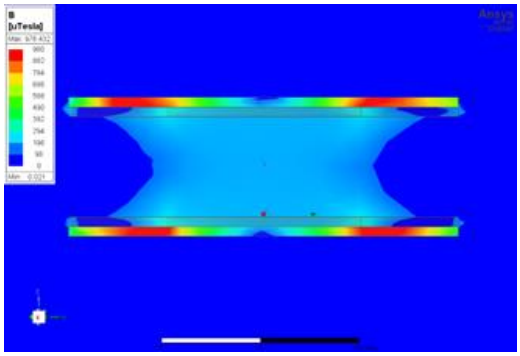

Fig.5.5 The magnetic field produced by circular coils.

Fig.5.6 and 5.7 Relationship between misalignment in centimetres and angles compared to the coupling coefficient of a circular coil [10]. In Fig.5.6, the curve exhibits a linear decrease as the misalignment rises. In Fig.5.7, when the angular displacement rises, the coupling coefficient changes within a range from lower to higher bounds. The simulation model of a circular coil with varying numbers of turns for both the transmitting and receiving coils [14].

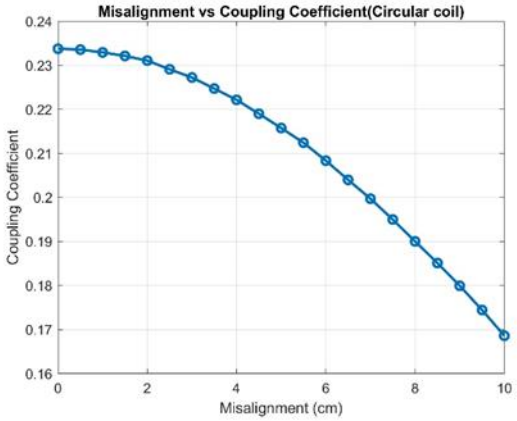

Fig.5.6. Circular coil coupling coefficient vs. misalignment.

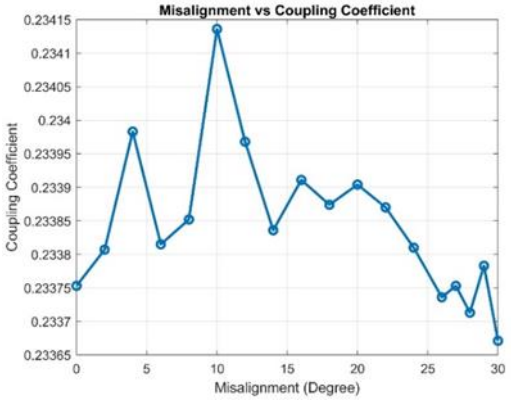

Fig.5.7 The relationship between misalignment in degrees and the coupling coefficient of a circular coil.

Chapter 6

Results and Discussion

5.1 Three Phase WPT system with Active Front End Rectifier

In order to validate the simulated results, the proposed topology of the Wireless EV charging as depicted in the Fig.6.1 having the waveform of the grid voltage (Fig.6.2a) exhibits a consistent sinusoidal pattern with a frequency of 50Hz, which varies depending on the geographical location. This observation suggests that the power supply grid is delivering a reliable and steady source of electricity.

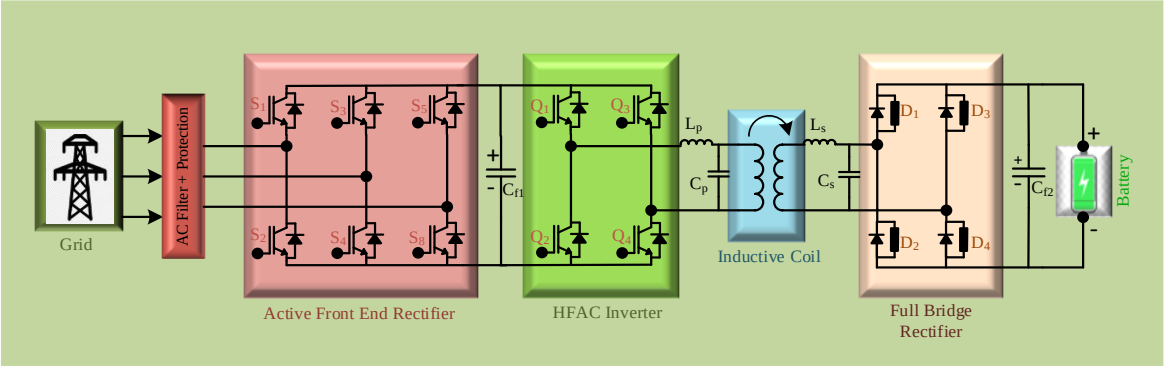

Fig.6.1 EV charger topology with primary and secondary charging stations

The current waveform (Fig.6.2b) exhibits the consumption of reactive power. Ideally, the system should monitor the grid voltage in order to enhance Power Factor (PF) and mitigate harmonic distortion. The V_{DC} link of AFE as shown in Fig.6.2c the DC link voltage waveform. A stable flat line indicates a well-regulated voltage, matching the 800V desired DC voltage. Any changes in the AFE output might point to variations in the load or input grid supply.

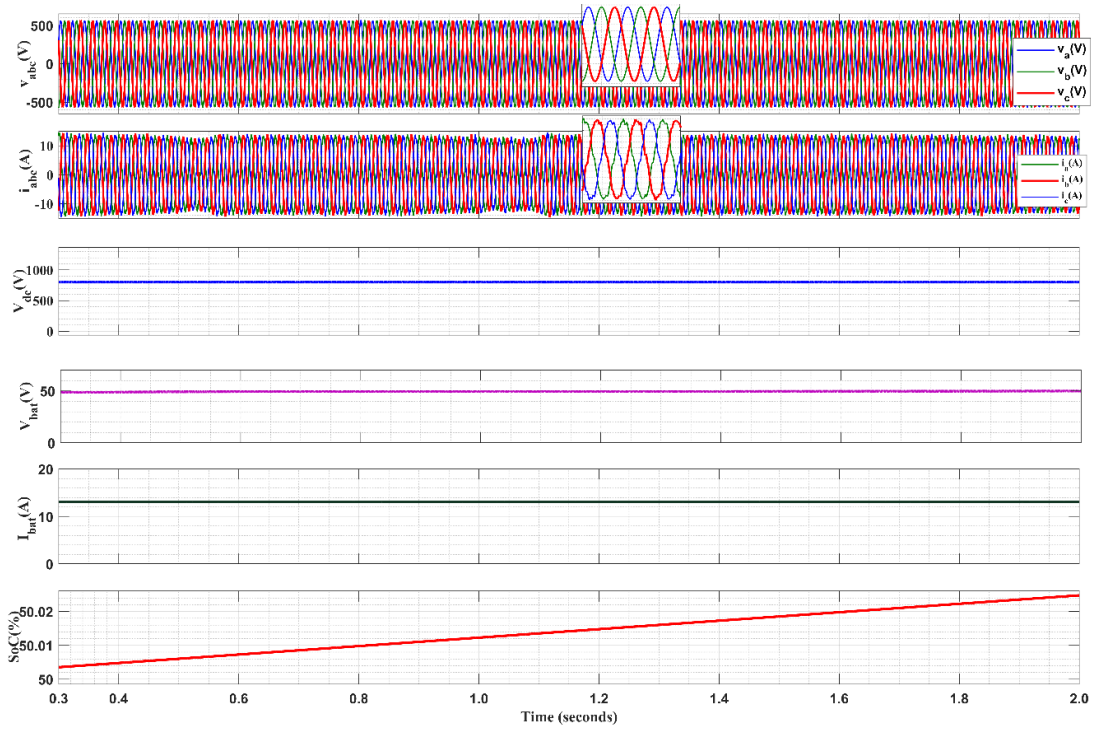

Fig.6.2(a) Grid voltage(top), (b)grid current, (c) V_{DC} -link (AFE), (d) battery voltage, (e)battery current, (f) State of charge of battery(bottom)

The battery voltage waveform (Fig.6.2d) initially rises as the battery starts to charge, then becomes stable once it reaches its rated voltage of 48V. This behaviour is expected as most batteries employ a constant voltage charging methodology.

The battery charging simulation offered successful and efficient charging of the lead-acid battery. The results of the simulation indicate that the charging voltage remains within the recommended range of 48V. Fig.6.2 illustrates the State of Charge (SoC%) of the battery, which serves as an indicator for the charging operation of the electric vehicle (EV) battery using the proposed topology of a wireless charger.

5.2 Single phase WPT System with Diode bridge Rectifier

The proposed circuit diagram's simulation indicates that power is transferred via the coil's inductive coupling. Fig. 6.3 shows a single-phase power supply that is fed from the grid.

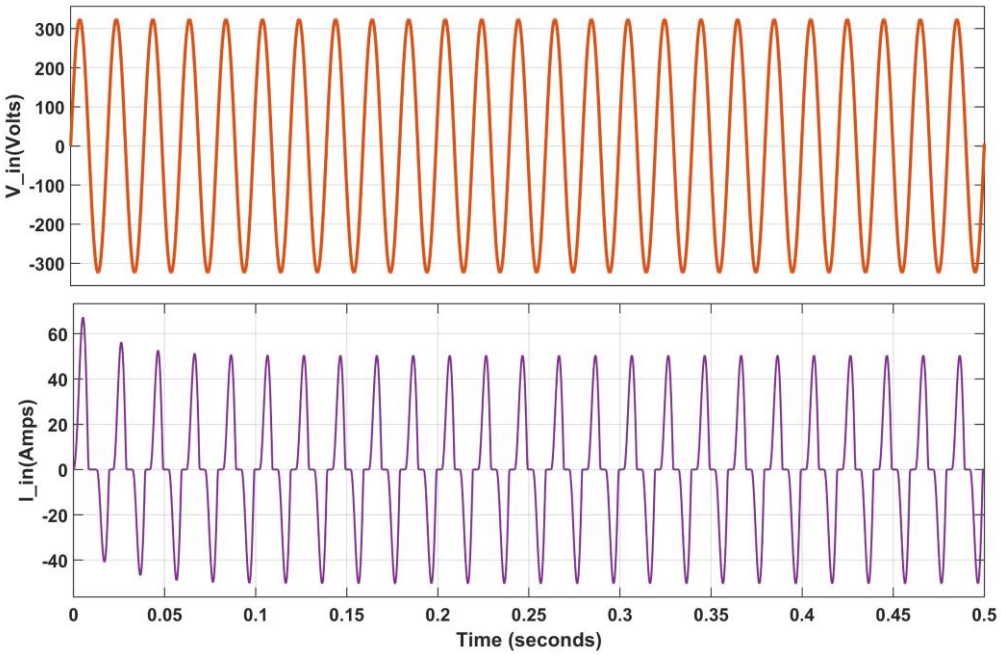

Fig.6.3 Input Voltage and Input current

The circuit diagram depicts the input of a single-phase power supply into the diode bridge rectifier, accompanied by an LC filter at the output. This configuration transforms the alternating current (AC) voltage into direct current (DC) voltage. In addition, a high-frequency inverter is linked to the dc-link capacitor of the diode bridge rectifier. The high frequency inverter converts the direct current (DC) input into alternating current (AC) with a frequency of 40 kHz. The AC signal is subsequently provided to the primary inductive coil, as depicted in Fig. 6.4

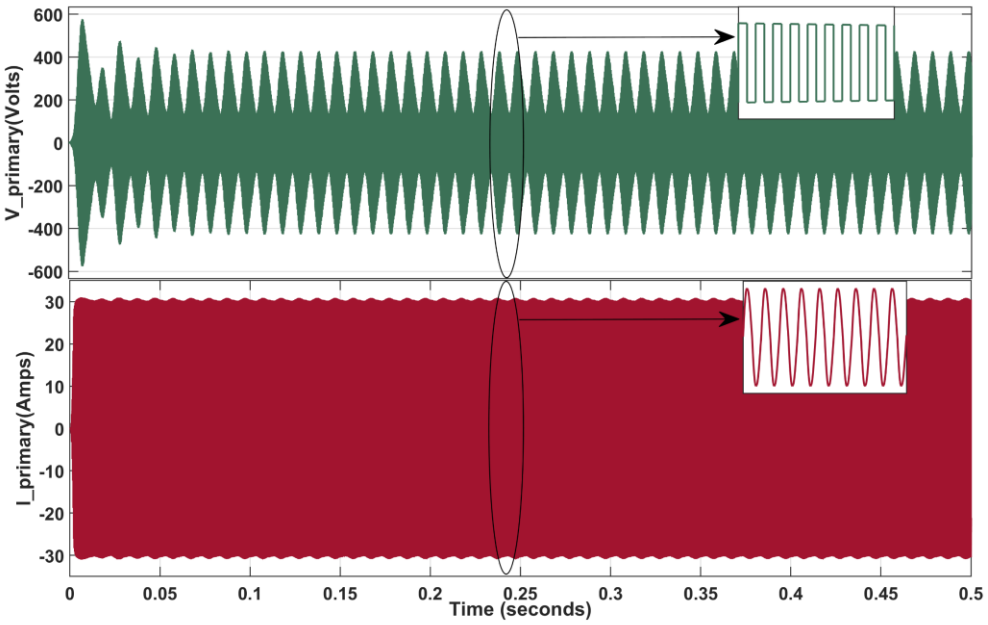

Fig.6.4 Primary Side coil voltage and Current

The primary inductive coil initiates the transfer of power using magnetic means, whereas the secondary inductive coil receives this power without the need for physical wiring, as depicted in Fig 6.5

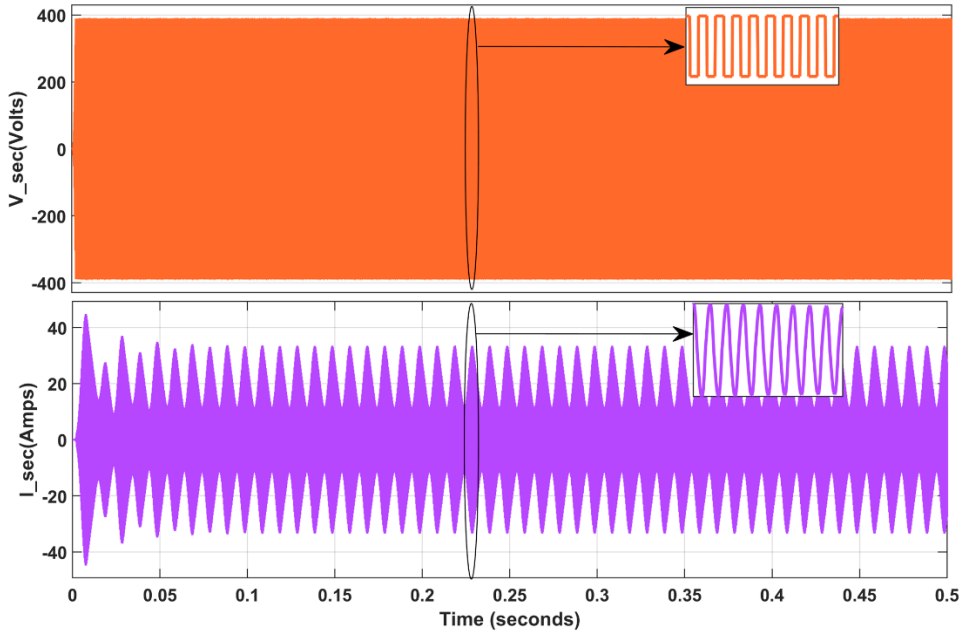

Fig. 6.5 Secondary Side coil voltage and Current

High frequency alternating current (HFAC) is the form of wireless power received by the primary coil. A diode bridge rectifier is used to transform it into DC, or direct current. Finally, the battery is connected to the DC power source via the bridge

rectifier's DC-link capacitor. The battery's charge level is increased during this charging procedure, as seen in Fig. 6.6 and Fig. 6.7.

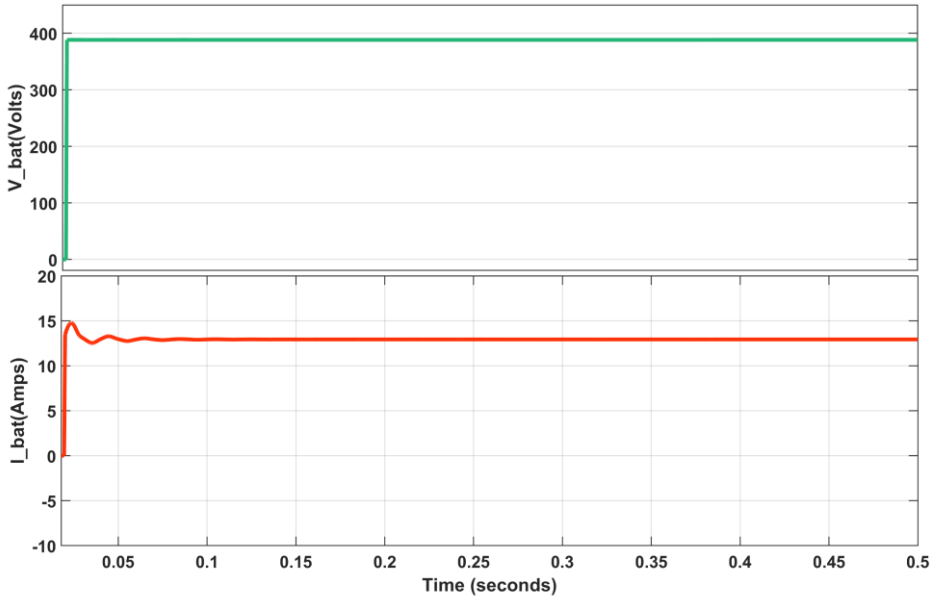

Fig.6.6 Battery Voltage and current

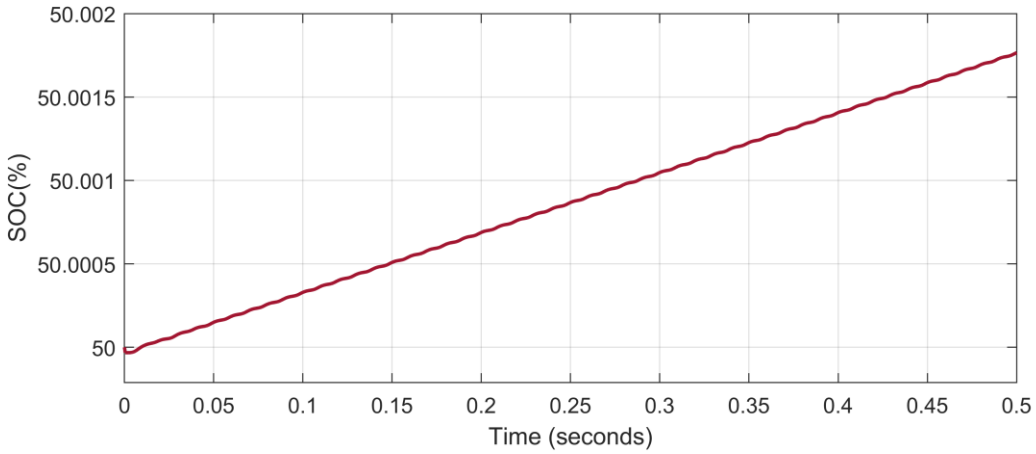

Fig.6.7 State of charge (SOC) of the Battery

Chapter 7

Conclusions and Future Scope

The investigation of wireless Electric Vehicle (EV) charging methods highlights a groundbreaking advancement in our approach to powering our automobiles. This new three-phase wireless charging system exemplifies a harmonious integration of effectiveness, security, and ease, establishing it as a leading contender in the forthcoming realm of electric vehicle charging solutions. The core of this groundbreaking method is in its capacity to sustain a consistent link to the energy supply, guaranteeing a seamless transformation from alternating current (AC) to direct current (DC) power. Ensuring a dependable DC connection voltage is crucial since it directly affects the efficiency of battery charging operations.

The success of this system relies on the implementation of the Active Front End (AFE) technology, which has a crucial function in maintaining the stability of the DC voltage. This steadiness is not just a technological accomplishment, but also the fundamental basis on which the entire charging process is improved. The detectable patterns of voltage and current in the battery during the process of charging provide support for the notion that the system is functioning as intended. An unmistakable indication of this achievement is the State of Charge (SoC) reaching 100%, which unequivocally demonstrates a battery that has been fully charged using effective and deliberate procedures.

This paper explores the intricacies of wireless power transfer (WPT), with a specific emphasis on the significant influence of coil design. By analyzing factors such as coil form, number of turns, frequency, distance between coils, and material qualities, one can get insights into the complex process of optimizing efficiency while minimizing loss. The results indicate that square coils, despite their straightforward design, may encounter efficiency difficulties as a result of alignment problems. On the other hand, circular coils, albeit having a higher inductance, are similarly susceptible to decreased efficiency in the event of misalignment.

An impressive accomplishment of this novel charging topology is its capacity to transfer 5kW of power wirelessly, showcasing an outstanding coil efficiency of

94.09%. The amount of efficiency demonstrated by the system not only emphasizes its usefulness, but also showcases its ability to minimize environmental impacts by lowering energy waste.

Nevertheless, the task of aligning coils remains a continuous domain for pioneering advancements. Enhancing alignment technology could greatly improve the overall efficiency of the charging system, as electric vehicles (EVs) may not always be perfectly positioned in relation to the charging infrastructure. Further research and development should focus on exploring the potential of incorporating dynamic alignment solutions that can adapt to different vehicle orientations.

In addition to its technical advantages, the sociological advantages of this wireless charging technology are significant. By providing a plug-and-charge solution, this technology streamlines the process of charging electric vehicles, which might potentially expedite the widespread use of electric vehicles by making them more attractive to a wider range of people. The simplicity and ease of this technology could serve as a decisive factor for numerous prospective EV consumers, transforming it into more than merely a charging development, but also a driving force for altering vehicle usage and ownership patterns.

Overall, the creation of the three-phase wireless EV charging system is a noteworthy achievement in the pursuit of improved, user-centric electric vehicle infrastructure. This technology overcomes significant obstacles such as power stability, coil efficiency, and alignment, while simultaneously meeting the practical requirements of users. As a result, it facilitates the broader adoption and utilization of electric vehicles. The quest for optimum wireless charging solutions encompasses not only technological progress but also the advancement of a sustainable future in transportation.

References

[1]. A N. Tesla, “Apparatus for transmitting electrical energy.” Google Patents, 01-Dec-1914.

[2]. A. Triviño-Cabrera, J. C. Quiró, J. M. González-González and J. A. Aguado, "Optimized Design of a Wireless Charger Prototype for an e-Scooter," *in IEEE Access*, vol. 11, pp. 33014-33026, 2023, doi: 10.1109/ACCESS.2023.3243958.

[3]. A. A. S. Mohamed, A. A. Marim and O. A. Mohammed, "Magnetic Design Considerations of Bidirectional Inductive Wireless Power Transfer System for EV Applications," in *IEEE Transactions on Magnetics*, vol. 53, no. 6, pp. 1-5, June 2017, Art no. 8700105, doi: 10.1109/TMAG.2017.2656819.

[4]. N. Fu, J. Deng, Z. Wang, W. Wang and S. Wang, "A Hybrid Mode Control Strategy for LCC–LCC- Compensated WPT System with Wide ZVS Operation," in *IEEE Transactions on Power Electronics*, vol. 37, no. 2, pp. 2449-2460, Feb. 2022, doi: 10.1109/TPEL.2021.3108637

[5]. L. Li, H. Liu, H. Zhang and W. Xue, "Efficient Wireless Power Transfer System Integrating With Metasurface for Biological Applications," in *IEEE Transactions on Industrial Electronics*, vol. 65, no. 4, pp. 3230-3239, April 2018, doi: 10.1109/TIE.2017.2756580.

[6]. Y. Li, J. Zhao, Q. Yang, L. Liu, J. Ma and X. Zhang, "A Novel Coil with High Misalignment Tolerance for Wireless Power Transfer," *in IEEE Transactions on Magnetics*, vol. 55, no. 6, pp. 1-4, June 2019, Art no. 2800904, doi: 10.1109/TMAG.2019.2904086.

[7]. Y. Zhang et al., "Integration of Onboard Charger and Wireless Charging System for Electric Vehicles with Shared Coupler, Compensation, and Rectifier," in *IEEE Transactions on Industrial Electronic*s, vol. 70, no. 7, pp. 7511-7514, July 2023, doi: 10.1109/TIE.2022.3204857.

[8]. A. R. K P and J. P, "Comparison of SRFT and ISOGI-QSG Control Algorithm for Grid Integrated SPV System," 2019 2nd International Conference on Intelligent Computing, Instrumentation and Control Technologies (ICICICT), Kannur, India, 2019, pp. 119-124, doi: 10.1109/ICICICT46008.2019.8993130

[9]. Erickson, R. W., Maksimovic, D. (2001). Fundamentals of Power Electronics. Springer.

[10]. Hussain, I.; Woo, D.-K. Simplified Mutual Inductance Calculation of Planar Spiral Coil for Wireless Power Applications. *Sensors* 2022, *22*, 1537. https://doi.org/10.3390/s22041537.

[11]. E. -S. Jun, S. Kwak and T. Kim, "Performance Comparison of Model Predictive Control Methods for Active Front End Rectifiers," in *IEEE Access*, vol. 6, pp. 77272-77288, 2018, doi: 10.1109/ACCESS.2018.2881133.
[12]. A. Singh, G. Yadav and M. Singh, "Performance Analysis of 3-Phase Active Front End PWM Rectifier for Air-Core Two-Coil WPT System Configuration," 2023 9th IEEE India International Conference on Power Electronics (IICPE), SONIPAT, India, 2023, pp. 1-6, doi: 10.1109/IICPE60303.2023.10474683.
[13]. "Global EV Outlook Understanding the Electric Vehicle Landscape to 2020," 2013.
[14]. Tesla, "New Tesla Model S Now the Quickest Production Car in the World | Tesla." [Online]. Available: https://www.tesla.com/blog/new-teslamodel-s-now-quickest-production-car-world. [Accessed: 01-Jul-2017].
[15]. Tesla, "Charging | Tesla." [Online]. Available: https://www.tesla.com/charging. [Accessed: 01-Jul-2017].
[16]. Rob Matheson, "Making a wire-free future," MIT News, 2014. [Online]. Available: http://news.mit.edu/2014/making-wire-free-future-0710. [Accessed: 01-Jul-2017].
[17]. Tianjia Sun, Xiang Xie, and Zhihua Wang, Wireless Power Transfer for Medical Microsystems. Springer, 2013.
[18]. H. W. Chiu, M. L. Lin, C. W. Lin, I. H. Ho, W. T. Lin, P. H. Fang, Y. C. Li, Y. R. Wen, and S. S. Lu, "Pain control on demand based on pulsed radio-frequency stimulation of the dorsal root ganglion using a batteryless implantable CMOS SoC," IEEE Trans. Biomed. Circuits Syst., vol. 4, no. 6 Part 1, pp. 350–359, 2010.
[19]. Ping Si, a P. Hu, S. Malpas, and D. Budgett, "A frequency control method for regulating wireless power to implantable devices.," Biomed. circuits Syst., vol. 2, no. 1, pp. 22–9, 2008.
[20]. Z. D. Boren, "There are officially more mobile devices than people in the world," The Independent, 2014. [Online]. Available: http://www.independent.co.uk/life-style/gadgets-and-tech/news/thereare-officially-more-mobile-devices-than-people-in-the-world9780518.html. [Accessed: 01-Jul-2017].
[21]. The Wireless Power Consortium, "Wireless Power The Qi Wireless Power Transfer System Power Class 0 Specification Parts 1 and 2 : Interface Definitions," 2016.
[22]. Geoff Gordon, "Introducing Quick Charge 3.0: next-generation fast charging technologyQualcomm,"2015.[Online].Available:https://www.qualcomm.com/news/onq/2015/09/14/introducing-quickcharge-30-next-generation-fast-charging-technology. [Accessed: 01-Jul2017].
[23]. Universal Serial Bus, "USB.org - USB Power Delivery." [Online]. Available: http://www.usb.org/developers/powerdelivery/. [Accessed: 01-Jul-2017].
[24]. AirFuel Alliance, "AirFuel Alliance - About." [Online].Available:http://www.airfuel.org/. [Accessed: 01-Jul-2017].

[25]. A. Kurs, A. Karalis, R. Moffatt, J. D. Joannopoulos, P. Fisher, and M. Soljačić, "Wireless Power Transfer via Strongly Coupled Magnetic Resonances," Science (80-.)., vol. 317, no. 5834, pp. 83–86, Jul. 2007.

[26]. W. Zhong, C. K. Lee, and S. Y. Ron Hui, "General analysis on the use of tesla's resonators in domino forms for wireless power transfer," IEEE Trans. Ind. Electron., vol. 60, no. 1, pp. 261–270, 2013.

[27]. T. Sun, X. Xie, G. Li, Y. Gu, Y. Deng, and Z. Wang, "A two-hop wireless power transfer system with an efficiency-enhanced power receiver for motion-free capsule endoscopy inspection," IEEE Trans. Biomed. Eng., vol. 59, no. 12 PART2, pp. 3247–3254, 2012.

[28]. H. H. Wu, A. Gilchrist, K. D. Sealy, and D. Bronson, "A High Efficiency 5 kW Inductive Charger for EVs Using Dual Side Control," IEEE Trans. Ind. Informatics, vol. 8, no. 3, pp. 585–595, Aug. 2012.

[29]. S. Li, W. Li, J. Deng, T. D. Nguyen, and C. C. Mi, "A Double-Sided LCC Compensation Network and Its Tuning Method for Wireless Power Transfer," IEEE Trans. Veh. Technol., vol. 64, no. 6, pp. 2261–2273, 2015.

[30]. Brian Maffly, "U. of Utah shuttle system getting wireless electric bus -The Salt LakeTribune,"TheSaltLakeTribune,2012.[Online].Available:http://archive.sltrib.com/story.php?ref=/sltrib/news/54117488-78/bus-technology-electric-smith.html.csp. [Accessed: 01-Jul-2017].

[31]. The Korea Advanced Institute of Science and Technology, "Wireless Online Electric Vehicle, OLEV, runs inner city roads," PHYS ORG, 2013. [Online]. Available: https://phys.org/news/2013-08-wireless-onlineelectric-vehicle-olev.html. [Accessed: 01-Jul-2017].

[32]. Christina Farr, "Utah-based WAVE nabs $1.4M to bring wireless electric buses to a dozen cities (exclusive) | VentureBeat | Enterprise | by Christina Farr," 2013. [Online]. Available: https://venturebeat.com/2013/10/10/utah-based-wave-nabs-1-4m-to-bring-wireless-electric-buses-to-a-dozen-cities-exclusive/. [Accessed: 01-Jul-2017].

[33]. Wireless Power Consortium, "Wireless Power Consortium Members." [Online]. Available: https://www.wirelesspowerconsortium.com/member-list/. [Accessed: 01-Jul-2017].

[34]. AirFuel Alliance, "AirFuel Alliance Members." [Online]. Available: http://www.airfuel.org/home/our-members. [Accessed: 01-Jul-2017].

[35]. G. A. Covic and J. T. Boys, "Modern Trends in Inductive Power Transfer for Transportation Applications," IEEE J. Emerg. Sel. Top. Power Electron., vol. 1, no. 1, pp. 28–41, Mar. 2013.

[36]. M. Eghtesadi, "Inductive power transfer to an electric vehicle-analytical model," in 40th IEEE Conference on Vehicular Technology, pp. 100–104.

[37]. U. K. Madawala, J. Stichbury, and S. Walker, "Contactless power transfer with two-way communication," in 30th Annual Conference of IEEE Industrial Electronics Society, 2004. IECON 2004, vol. 3, pp. 3071–3075.

[38]. Chih-Jung Chen, Tah-Hsiung Chu, Chih-Lung Lin, and Zeui-Chown Jou, “A Study of Loosely Coupled Coils for Wireless Power Transfer,” IEEE Trans. Circuits Syst. II Express Briefs, vol. 57, no. 7, pp. 536–540, Jul. 2010.
[39]. C. K. Lee, W. X. Zhong, and S. Y. R. Hui, “Effects of Magnetic Coupling of Nonadjacent Resonators on Wireless Power Domino-Resonator Systems,” IEEE Trans. Power Electron., vol. 27, no. 4, pp. 1905–1916, Apr. 2012.
[40]. S. Li and C. C. Mi, “Wireless Power Transfer for Electric Vehicle Applications,” Emerging and Selected Topics in Power Electronics, IEEE Journal of, vol. 3, no. 1. pp. 4–17, 2015.
[41]. B. X. Nguyen, D. M. Vilathgamuwa, G. H. B. Foo, P. Wang, A. Ong, U. K. Madawala, and T. D. Nguyen, “An Efficiency Optimization Scheme for Bidirectional Inductive Power Transfer Systems,” IEEE Trans. Power Electron., vol. 30, no. 11, pp. 6310–6319, Nov. 2015.
[42]. U. K. Madawala and D. J. Thrimawithana, “A Bidirectional Inductive Power Interface for Electric Vehicles in V2G Systems,” Industrial Electronics, IEEE Transactions on, vol. 58, no. 10. pp. 4789–4796, 2011.
[43]. A. K. RamRakhyani, S. Mirabbasi, and M. Chiao, “Design and Optimization of Resonance-Based Efficient Wireless Power Delivery Systems for Biomedical Implants,” IEEE Trans. Biomed. Circuits Syst., vol. 5, no. 1, pp. 48–63, Feb. 2011.
[44]. R. Jegadeesan, S. Nag, K. Agarwal, N. V. Thakor, and Y.-X. Guo, “Enabling Wireless Powering and Telemetry for Peripheral Nerve Implants,” IEEE J. Biomed. Heal. Informatics, vol. 19, no. 3, pp. 958–970, May 2015.
[45]. R. Jegadeesan and Y.-X. Guo, “Modeling of wireless power transfer link for retinal implant,” in 2016 IEEE/ACES International Conference on Wireless Information Technology and Systems (ICWITS) and Applied Computational Electromagnetics (ACES), 2016, pp. 1–2.
[46]. R.-F. F. Xue, K.-W. W. Cheng, and M. Je, “High-efficiency wireless power transfer for biomedical implants by optimal resonant load transformation,” IEEE Trans. Circuits Syst. I Regul. Pap., vol. 60, no. 4, pp. 867–874, Apr. 2013.
[47]. V. T. Nguyen, S. H. Kang, J. H. Choi, and C. W. Jung, “Magnetic resonance wireless power transfer using three-coil system with single planar receiver for laptop applications,” IEEE Trans. Consum. Electron., vol. 61, no. 2, pp. 160–166, May 2015.
[48]. M. Dionigi, M. Mongiardo, and R. Perfetti, “Rigorous Network and Full Wave Electromagnetic Modeling of Wireless Power Transfer Links,” IEEE Trans. Microw. Theory Tech., vol. 63, no. 1, pp. 65–75, Jan. 2015.
[49]. J. Kim, H. Son, D. Kim, and Y. Park, “Optimal design of a wireless power transfer system with multiple self-resonators for an LED TV,” IEEE Trans. Consum. Electron., vol. 58, no. 3, pp. 775–780, Aug. 2012.
[50]. S. Y. Hui, “Planar Wireless Charging Technology for Portable Electronic Products and Qi,” Proc. IEEE, vol. 101, no. 6, pp. 1290–1301, Jun. 2013.
[51]. Jian Yin, Deyan Lin, Chi Kwan Lee, T. Parisini, and S. Y. Hui, “FrontEnd Monitoring of Multiple Loads in Wireless Power Transfer Systems Without

Wireless Communication Systems," IEEE Trans. Power Electron., vol. 31, no. 3, pp. 2510–2517, Mar. 2016.
[52]. C. G. Kim, D. H. Seo, J. S. You, J. H. Park, and B. H. Cho, "Design of a contactless battery charger for cellular phone," IEEE Trans. Ind. Electron., vol. 48, no. 6, pp. 1238–1247, 2001.
[53]. Y. Jang and M. M. Jovanović, "A contactless electrical energy transmission system for portable-telephone battery chargers," IEEE Trans. Ind. Electron., vol. 50, no. 3, pp. 520–527, 2003.
[54]. B. Choi, J. Nho, H. Cha, T. Ahn, and B. Choi, "Design and implementation of low-profile contactless battery charger using planar printed circuit board windings as energy transfer device," Industrial Electronics, IEEE Transactions on, vol. 51, no. 1. pp. 140–147, 2004.
[55]. E. Waffenschmidt, "Wireless power for mobile devices," in 2011 IEEE 33rd International Telecommunications Energy Conference (INTELEC), 2011, pp. 1–9.
[56]. C. Y. Huang, J. T. Boys, and G. A. Covic, "LCL pickup circulating current controller for inductive power transfer systems," IEEE Trans. Power Electron., vol. 28, no. 4, pp. 2081–2093, 2013.
[57]. H. L. Li, A. P. Hu, and G. A. Covic, "A Direct AC–AC Converter for Inductive Power-Transfer Systems," IEEE Trans. Power Electron., vol. 27, no. 2, pp. 661–668, Feb. 2012.
[58]. D. Kurschner, C. Rathge, and U. Jumar, "Design Methodology for High Efficient Inductive Power Transfer Systems With High Coil Positioning Flexibility," IEEE Trans. Ind. Electron., vol. 60, no. 1, pp. 372–381, Jan. 2013.
[59]. J. Kim, J. Kim, S. Kong, H. Kim, I.-S. Suh, N. P. Suh, D.-H. Cho, J. Kim, and S. Ahn, "Coil Design and Shielding Methods for a Magnetic Resonant Wireless Power Transfer System," Proc. IEEE, vol. 101, no. 6, pp. 1332–1342, Jun. 2013.
[60]. J. Shin, S. Shin, Y. Kim, S. Ahn, S. Lee, G. Jung, S.-J. Jeon, and D. H. Cho, "Design and Implementation of Shaped Magnetic Resonance Based Wireless Power Transfer System for Roadway-Powered Moving Electric Vehicles," IEEE Trans. Ind. Electron., vol. 61, no. 3, pp. 1179–1192, 2014.
[61]. J. Huh, S. W. Lee, W. Y. Lee, G. H. Cho, and C. T. Rim, "Narrow-Width Inductive Power Transfer System for Online Electrical Vehicles," IEEE Trans. Power Electron., vol. 26, no. 12, pp. 3666–3679, Dec. 2011.
[62]. J. M. Miller, O. C. Onar, C. White, S. Campbell, C. Coomer, L. Seiber, R. Sepe, and A. Steyerl, "Demonstrating dynamic wireless charging of an electric vehicle: The benefit of electrochemical capacitor smoothing," IEEE Power Electron. Mag., vol. 1, no. 1, pp. 12–24, 2014.
[63]. J. M. Miller, O. C. Onar, and M. Chinthavali, "Primary Side Power Flow Control of Wireless Power Transfer for Electric Vehicle Charging," IEEE J. Emerg. Sel. Top. Power Electron., vol. 3, no. 1, pp. 1–1, 2014.

[64]. J. M. Miller, P. T. Jones, J. M. Li, and O. C. Onar, “ORNL experience and challenges facing dynamic wireless power charging of EV’s,” IEEE Circuits Syst. Mag., vol. 15, no. 2, pp. 40–53, 2015.

[65]. O. C. Onar, J. M. Miller, S. L. Campbell, C. Coomer, C. P. White, and L. E. Seiber, “A novel wireless power transfer for in-motion EV/PHEV charging,” Conf. Proc. - IEEE Appl. Power Electron. Conf. Expo. - APEC, pp. 3073–3080, 2013.

[66]. S. Zhou and C. Mi, “Multi-Paralleled LCC Reactive Power Compensation Networks and Its Tuning Method for Electric Vehicle Dynamic Wireless Charging,” IEEE Transactions on Industrial Electronics, vol. PP, no. 99. p. 1, 2015.

[67]. C.-S. Wang, G. A. Covic, and O. H. Stielau, “Power transfer capability and bifurcation phenomena of loosely coupled inductive power transfer systems,” Industrial Electronics, IEEE Transactions on, vol. 51, no. 1. pp. 148–157, 2004.

[68]. G. A. Covic and J. T. Boys, “Inductive Power Transfer,” Proc. IEEE, vol. 101, no. 6, pp. 1276–1289, Jun. 2013.

[69]. M. Borage, S. Tiwari, and S. Kotaiah, “Analysis and design of an LCL-T resonant converter as a constant-current power supply,” IEEE Trans. Ind. Electron., vol. 52, no. 6, pp. 1547–1554, 2005.

[70]. B. Sharp and H. Wu, “Asymmetrical voltage-cancellation control for LCL resonant converters in inductive power transfer systems,” Conf. Proc. -IEEE Appl. Power Electron. Conf. Expo. - APEC, pp. 661–666, 2012.

[71]. N. A. Keeling, G. A. Covic, and J. T. Boys, “A unity-power-factor IPT pickup for high-power applications,” IEEE Trans. Ind. Electron., vol. 57, no. 2, pp. 744–751, 2010.

[72]. H. H. Wu, A. Gilchrist, K. Sealy, P. Israelsen, and J. Muhs, “Design of Symmetric Voltage Cancellation Control for LCL converters in Inductive Power Transfer Systems,” 2011 IEEE Int. Electr. Mach. Drives Conf. IEMDC 2011, pp. 866–871, 2011.

[73]. D. Voglitsis, G. Tsengenes, and P. Bauer, “Inductive power transfer system with improved characteristics,” in 2014 IEEE Transportation Electrification Conference and Expo (ITEC), 2014, pp. 1–8.

[74]. W. Li, C. C. Mi, S. Li, J. Deng, T. Kan, and H. Zhao, “Integrated LCC Compensation Topology for Wireless Charger in Electric and Plug-in Electric Vehicles,” IEEE Trans. Ind. Electron., pp. 1–1, 2014.

[75]. J. T. Boys, G. A. Covic, and A. W. Green, “Stability and control of inductively coupled power transfer systems,” IEE Proc. - Electr. Power Appl., vol. 147, no. 1, p. 37, Jan. 2000.

[76]. A. Mahesh, B. Chokkalingam and L. Mihet-Popa, "Inductive Wireless Power Transfer Charging for Electric Vehicles–A Review," *in IEEE Access*, vol. 9, pp. 137667-137713, 2021, doi: 10.1109/ACCESS.2021.3116678.

[77]. A. Ahmad, M. S. Alam and R. Chabaan, "A Comprehensive Review of Wireless Charging Technologies for Electric Vehicles," in *IEEE Transactions on*

Transportation Electrification, vol. 4, no. 1, pp. 38-63, March 2018, doi: 10.1109/TTE.2017.2771619.

[78]. S. Li, F. Li, R. Zhang, C. Tao and L. Wang, "Accurate Modeling, Design and Load Estimation of LCC-S based WPT system with a wide range of load," in *IEEE Transactions on Power Electronics*, doi: 10.1109/TPEL.2023.3279659.

[79]. A. A. S. Mohamed, D. Allen, T. Youssef and O. Mohammed, "Optimal design of high frequency H-bridge inverter for wireless power transfer systems in EV applications," *2016 IEEE 16th International Conference on Environment and Electrical Engineering (EEEIC),* Florence, Italy, 2016, pp. 1-6, doi: 10.1109/EEEIC.2016.7555646.

[80]. A. Ramezani and M. Narimani, "Optimized Electric Vehicle Wireless Chargers with Reduced Output Voltage Sensitivity to Misalignment," in *IEEE Journal of Emerging and Selected Topics in Power Electronics*, vol. 8, no. 4, pp. 3569-3581, Dec. 2020, doi: 10.1109/JESTPE.2019.2958932.

List of Publication

1. **9th IEEE India International Conference on Power Electronics (IICPE-2023)**

   Title: Performance Analysis of 3-phase Active Front End PWM Rectifier for Air-Core Two-Coil WPT System Configuration
   (https://doi.org/10.1109/IICPE60303.2023.10474683)

2. **First International Conference on Recent Advances in Smart Energy Systems & Intelligent Automation (RASESIA 2024)**

   Title: Investigation of Misalignment Response in Inductive Power Transfer Technology to Boost Efficiency and Tolerance in Electric Vehicles Charging (**Paper Accepted)**

PAPER NAME

Anurag_Thesis_01.pdf

WORD COUNT

13900 Words

CHARACTER COUNT

75230 Characters

PAGE COUNT

61 Pages

FILE SIZE

2.2MB

SUBMISSION DATE

May 31, 2024 1:23 PM GMT+5:30

REPORT DATE

May 31, 2024 1:24 PM GMT+5:30

13% Overall Similarity

The combined total of all matches, including overlapping sources, for each database.

- 7% Internet database
- 5% Publications database
- Crossref database
- Crossref Posted Content database
- 6% Submitted Works database

Excluded from Similarity Report

- Bibliographic material
- Small Matches (Less then 10 words)

IEEE

IICPE 2023

9TH IEEE INDIA INTERNATIONAL CONFERENCE ON POWER ELECTRONICS

(28th – 30th November 2023)

Deenbandhu Chhotu Ram University of Science & Technology, Murthal, Haryana, India

This certificate of Participation/Presentation is awarded to

Dr./Mr./Ms. Anurag Singh from DTU, Delhi

has attended the conference and presented paper entitled Performance Analysis of 2-Phase Active Front End PWM Rectifier for Air-Core Two-Coil WPT System Configuration

authored by Anurag Singh, Gaurav Yadav; Mukhtiar Singh in the 9th IEEE India International Conference on Power Electronics held at Deenbandhu Chhotu Ram University of Science & Technology, Murthal, Haryana, India from 28th – 30th November 2023.

Dr. D.K Jain
General Chair

Dr. Surender Dahiya
General Chair

Gmail Anurag Singh <sanurag1012@gmail.com>

Accept

1 message

Microsoft CMT <email@msr-cmt.org> 27 May 2024 at 18:37
Reply-To: Dr Shivam <shivam@nitkkr.ac.in>
To: Anurag Singh <Sanurag1012@gmail.com>

Dear Anurag,
We are pleased to inform you that your manuscript entitled "Investigation of Misalignment Response in Inductive Power Transfer Technology to Boost Efficiency and Tolerance in Electric Vehicles Charging" has been provisionally accepted for presentation in First International Conference on Recent Advances in Smart Energy Systems & Intelligent Automation.

To ensure that your paper is submitted to SPRINGER for publication in the Scopus-indexed "Lecture Notes in Electrical Engineering (LNEE)", please follow the instructions below:
1. You have to incorporate the suggestions and comments of reviewers while preparing the final camera-ready Paper (in an ms-word/latex format as per the Springer-LNEE template). The reviews can be found in your Microsoft CMT account.
The Final camera-ready paper should be prepared in the SPRINGER-LNEE template only which can be downloaded from https://www.springer.com/gp/authors-editors/conference-proceedings/conference-proceedings-guidelines. Authors are also reminded that LNEE has a very strong anti-plagiarism policy for conference papers (less than 20% similarity index with 8 words limit setting in the Turnitin).

2. Please prepare a response sheet consisting of a point-wise response to the reviewers' comments and mention where the changes have been incorporated in the camera-ready paper.

3. You have to complete the registration process by May 30, 2024 – details will be available soon at https://www.rasesia2024.com/ and same will be emailed to you.

4. You have to submit the copyright form – the information will be communicated later on.

The Conference Organizers reserve the right not to include the paper in the conference proceedings if it is not compliant with RASESIA 2024 formatting instructions or similarity index.

Thank you for considering the RASESIA 2024 to present the results of your research. For any queries, please feel free to contact us at https://www.rasesia2024.com/

Please refer to the website https://www.rasesia2024.com/" for further updates about the conference.

We look forward to meeting you (online/offline) Hybrid Mode at RASESIA 2024.

Kindly do the registration as soon as possible (the same information has been uploaded on the conference website home page).

Best regards,
Program Committee, RASESIA 2024